Adaptive neural network-based robust H_∞ tracking control of a quadrotor UAV under wind disturbances

Zakaria Bellahcene* and
Mohamed Bouhamida

Key Laboratory of Automatics Vision and Intelligent Control Systems,
Department of Automatic,
University of Science and Technology of Oran,
USTO-MB BP 1505 El M'naouer, 31000 Oran, Algeria
Email: zakaria.bellahcene@univ-usto.dz
Email: mohammedbouhamida31@gmail.com
*Corresponding author

Mouloud Denai

University of Hertfordshire,
Hatfield, UK
Email: m.denai@herts.ac.uk

Khaled Assali

Key Laboratory of Automatics Vision and Intelligent Control Systems,
Department of Automatic,
University of Science and Technology of Oran,
USTO-MB BP 1505 El M'naouer, 31000 Oran, Algeria
Email: assali_khaled@yahoo.fr

Abstract: The paper deals with the stabilisation and trajectory tracking control of an autonomous quadrotor helicopter system in the presence of wind disturbances. The proposed adaptive tracking controller uses radial basis function neural networks (RBF NNs) to approximate unknown nonlinear functions in the system. Two controllers are proposed in this paper to handle the modelling errors and external disturbances: H_∞ adaptive neural controller H_∞-ANC and H_∞-based adaptive neural sliding mode controller H_∞-ANSMC. The design approach combines the robustness of sliding mode control (SMC) with the ability of H_∞ to deal with parameter uncertainties and bounded disturbances. Furthermore, the RBF models are derived using Lyapunov stability analysis. The simulation results show that H_∞-ANSMC is able to eliminate the chattering phenomenon, reject perturbation mismatch and leads to a better performance than H_∞-ANC. A comparative simulation study between the proposed controllers is presented and the results are discussed.

Keywords: adaptive tracking; H_∞ control; quadrotor control; neural networks; sliding mode control; SMC.

Reference to this paper should be made as follows: Bellahcene, Z., Bouhamida, M., Denai, M. and Assali, K. (xxxx) 'Adaptive neural network-based robust H_∞ tracking control of a quadrotor UAV under wind disturbances', *Int. J. Automation and Control*, Vol. x, No. x, pp.xxx–xxx.

Biographical notes: Zakaria Bellahcene is currently a PhD student at the Department of Automatic Control Engineering, University of Science and the Technology of Oran, Algeria. He received his Engineering in Automatic Control in 2008 and Magister in 2013. His research interests include aerial robotics, linear and nonlinear control, analysis and design of intelligent systems.

Mohamed Bouhamida received his Engineering in Electronics in 1982, Magister in 1992 and PhD in Automatics in 2006 from the University of Sciences and Technology of Oran 'Mohamed Boudiaf', Algeria. After graduation, he joined the Automatic Department of University of Sciences and Technology of Oran. He was a Professor and the Director of Automatique Laboratory at the University of Sciences and Technology of Oran (AVCIS). His research interests include electric machine drives, power electronics and process control.

Mouloud Denai is a Senior Lecturer in Electric Power and Control. He graduated from the University of Science and Technology of Algiers and Ecole Nationale Polythechnique of Algiers, Algeria in Electrical Engineering and he received his PhD in Control Engineering from the University of Sheffield, UK. He worked for the University of Science and Technology of Oran, Algeria in 2004 and in the University of Sheffield, UK from 2004 to 2010. He worked for Teesside University from 2010 to 2014. He is currently working in the School of Engineering and Technology, University of Hertfordshire, UK.

Khaled Assali is currently a PhD student at the Department of Automatic Control Engineering, University of Science and the Technology of Oran, Algeria. He received his Magister in 2011. His research interests include analysis and synthesis of nonlinear systems, robust control, adaptive control.

This paper is a revised and expanded version of a paper entitled [title] presented at [name, location and date of conference].

1 Introduction

Unmanned aerial vehicles (UAVs) are receiving considerable attention these recent years and their design and control are still an active area of research. The quadrotor continues to be the most widely used UAV in both defense and civilian applications. Compared with traditional helicopters (Maiti et al., 2018), quadrotors have several advantages such as low cost and can be easily controlled by varying the speed of the rotors. Many approaches have been proposed to control the quadrotor helicopter and some strategies have been developed to solve path-following problems. Initially, the quadrotor has been controlled using a three degrees of freedom (DOF) model structure

by referring to Tayebi and McGilvray (2006). Because of the inherent nonlinearity in the system, feedback linearisation approach is adopted by Lanzon et al. (2014) to design the controller. In the last few years, adaptive tracking control of nonlinear systems has received much attention and a significant progress has been made (Mohammadi and Shahri, 2013). However, precise models of quadrotors are difficult to obtain. One potential way to address this problem is to use computational intelligence-based control methods such as neural networks control used by Wang et al. (2012) and Chen et al. (2015). Basri et al. (2015) proposed an intelligent back-stepping (BS) controller based on the radial basis function neural network (RBF NNs) as perturbation approximators. The BS controller parameters are optimised based on the particle swarm optimisation algorithm. Other control approaches can be found in the literature, such as fuzzy logic control (Talha et al., 2018) and learning-based control (Zhang et al., 2015). Sliding mode and high-order sliding mode-based observers have also been used by Besnard et al. (2012) and Shakev et al. (2015) to estimate unmeasured states and the effects of external disturbances such as wind and noise. Some results addressing the stability and performance analysis of quadrotors are discussed by Ozbek et al. (2015). The paper presents a comprehensive performance evaluation of several controllers including proportional-integral-derivative control, sliding mode control (SMC), backstepping control, feedback linearisation-based control and fuzzy control. Most of the robust controllers proposed for UAV control are based on H_∞ control because its effective design methodology which offers robustness and ease of implementation. Mokhtari et al. (2005) presented mixed robust feedback linearisation with GH_∞ controller. Amin and Aijun (2017) proposed a mixed sensitivity H_∞ controller for attitude control of a four-rotor hover vehicle. The mixed sensitivity approach allows shaping the sensitivity (S) and complementary sensitivity functions (T) of the closed-loop system.

Artificial neural networks (ANN) have been extensively used as nonlinear function approximators in control design of uncertain nonlinear systems due to their universal approximation capabilities (Chung and Scarselli, 1998; Boufadene et al., 2018). Thus, an ANN can be readily used to model the uncertainties in the quadrotor system dynamics. The basic concept of this scheme is that an ANN approximates the unknown dynamics so that the tracking performance of the system can be improved. As suggested by Yacef et al. (2012), quadrotor dynamics are represented in state-space form which is more convenient to implement the proposed approach.The dynamics of the quadrotor helicopter with parameter variations and external disturbances can be treated as an uncertain nonlinear system. So far, to the best of our knowledge, only a small number of studies have employed neural networks for quadrotor helicopter control design.

In this paper, the H_∞ tracking control design method is combined with adaptive neural SMC H_∞-ANSMC. RBF ANNs are used to approximate the unknown nonlinear functions of the nominal model of the quadrotor. Due to the existence of approximation errors of neural networks and external disturbance, H_∞ and sliding mode method as the robust controller to enhance system robustness and maintain boundedness are utilised. The adaptive law used to adjust the weights of the neural network model is derived from a suitable Lyapunov equation. This Lyapunov stability condition was then transformed into a linear matrix inequality (LMI) form and the H_∞-ANSMC design problem was solved subject to this LMI. The closed-loop system stability can be established based on Lyapunov stability criterion. The major contributions of the current study can be summarised as follows: neural networks are proposed to approximate the unknown nonlinear functions $f_{0i}(X)$ and $g_{0i}(X)$ which overcomes the need for an

accurate mathematical model of the system. Two robust adaptive neural networks-based sliding mode and H_∞ control strategies are proposed for quadrotor trajectory tracking with robustness against uncertainties and attenuation of wind gust disturbances. The undesirable effects of the chattering phenomena that usually occur in SMC have been reduced by using H_∞-ANSMC. The width of the chattering band has been significantly reduced in this method.

Using Lyapunov theory, it can be proved that the resulting closed-loop system is robustly stable and uniformly ultimately bounded (UUB) and the actual system output follows closely the desired output. The rest of the paper is organised as follows. In Section 2, the UAV dynamic model is presented in state-space form. In Section 3, the tracking control problem for aerial quadrotor system under uncertainties is introduced, and some preliminary results are presented. In Sections 4 and 5, the robust adaptive neural tracking control schemes based on H_∞ and H_∞-ANSMC methods are presented. Simulation results to illustrate the effectiveness of the proposed control schemes are presented in Section 6. Finally, some conclusions are drawn in Section 7.

2 Dynamic model of the quadrotor UAV

The quadrotor consists of four propellers in cross configuration where the pairs of rotors (1, 3) and (2, 4), turn in opposite directions to prevent the device from turning around itself Figure 1. Forward motion is achieved by increasing the speed of the rear rotor while simultaneously reducing the forward rotor by the same amount. Left and right motions work in the same way. Yaw command is performed by accelerating the two clockwise turning rotors while decelerating the counter-clockwise turning rotors. The equations describing the altitude and the attitude motions of a quadrotor UAV are basically those of a rotating rigid body with six DOF. Consider the two main reference frames, the earth fixed inertial reference frame $E^b\left(o^b, \overline{e_1^b}, \overline{e_2^b}, \overline{e_3^b}\right)$ and the body fixed reference frame $E^m\left(o^m, \overline{e_1^m}, \overline{e_2^m}, \overline{e_3^m}\right)$ shown in Figure 1. The absolute position of the quadrotor is described by $\overline{o^b o^m} = \xi = [x, y, z]^T$ and its attitude by the three Euler's angles $\alpha = [\phi, \theta, \psi]$.

Assumption 1: The yaw, pitch and roll angles are restricted to $-\pi < \psi < \pi$, $-\pi/2 \leq \theta \leq \pi/2$ and $-\pi/2 \leq \phi \leq \pi/2$.

Figure 1 Structure of the quadrotor UAV

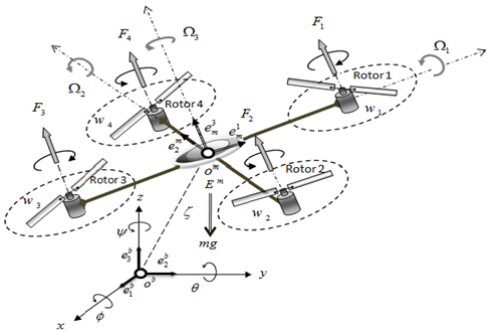

By using the formalism of Newton-Euler (position and orientation dynamic), a good controller should be able to reach a desired position and a desired yaw angle while guaranteeing stability of the pitch and roll angles. Many works on quadrotors modelling have been reported in the literature. In this paper, the quadrotor state space model described in Yacef et al. (2012) is used for the design of the controller. The dynamic model of a quadrotor is written state-space as

$$\dot{x} = f(X, u) \tag{1}$$

with the following state vector X and input vector u

$$\begin{array}{l} X = [x_{11}, x_{12}, ..., x_{61}, x_{62}]^T \in \Re^{12} \\ x_{11} = \phi, x_{12} = \dot{\phi}, x_{21} = \theta, x_{22} = \dot{\theta} \\ x_{31} = \psi, x_{32} = \dot{\psi}, x_{41} = z, x_{42} = \dot{z} \\ x_{51} = x, x_{52} = \dot{x}, x_{61} = y, x_{62} = \dot{y} \end{array} \tag{2}$$

where $u = [u_1, u_2, u_3, u_4]^T$ are the control inputs of the system which are written in terms of the angular velocities of the four rotors as follows

$$\begin{pmatrix} u_1 \\ u_2 \\ u_3 \\ u_4 \end{pmatrix} = \begin{pmatrix} 0 & -lb & 0 & lb \\ -lb & 0 & lb & l0 \\ d & -d & d & -d \\ b & b & b & b \end{pmatrix} \begin{pmatrix} \omega_1^2 \\ \omega_2^2 \\ \omega_3^2 \\ \omega_4^2 \end{pmatrix} \tag{3}$$

where b and d denote respectively the thrust and drag coefficients, l is the arm length of the quadrotor. With $\Omega_r = \omega_1 - \omega_2 + \omega_3 - \omega_4$. Equation (3) can be written in the following form

$$u = \Theta F \tag{4}$$

The forces are calculated from the following equation

$$F = \begin{pmatrix} F_1 \\ F_2 \\ F_3 \\ F_4 \end{pmatrix} = \begin{pmatrix} 0 & -l & 0 & l \\ -l & 0 & l & 0 \\ d/b & -d/b & d/b & -d/b \\ 1 & 1 & 1 & 1 \end{pmatrix}^{-1} \begin{pmatrix} u_1 \\ u_2 \\ u_3 \\ u_4 \end{pmatrix} = \Theta^{-1} u \tag{5}$$

where $F_j = b\omega_j^2$, j = (1, ..., 4) is the force generated by the j^{th} rotor. The nonlinear function can be expressed in state-space form as

$$f(X, u) = \begin{pmatrix} x_{12} \\ a_0 x_{22} x_{32} + a_1 \Omega_r x_{22} + a_2 x_{12}^2 + b_0 u_1 + d_1 \\ x_{22} \\ a_3 x_{12} x_{32} + a_4 \Omega_r x_{12} + a_5 x_{22}^2 + b_1 u_2 + d_2 \\ x_{32} \\ a_6 x_{12} x_{22} + a_7 x_{32}^2 + b_2 u_3 + d_3 \\ x_{42} \\ a_{10} x_{42} - g + b_3 \cos x_{11} \cos x_{21} u_4 + d_4 \\ x_{52} \\ a_8 x_{52} + b_3 u_4 u_5 + d_5 \\ x_{62} \\ a_9 x_{62} + b_3 u_4 u_6 + d_6 \end{pmatrix} \tag{6}$$

$$\begin{cases} a_0 = \frac{(I_y - I_z)}{I_x}, a_1 = -\frac{J_r}{I_x}, a_2 = -\frac{K_{fax}}{I_x} \\ a_3 = \frac{(I_z - I_x)}{I_y}, a_4 = +\frac{J_r}{I_y}, a_5 = -\frac{K_{fay}}{I_y} \\ a_6 = \frac{(I_x - I_y)}{I_z}, a_7 = -\frac{K_{faz}}{I_z}, a_8 = -\frac{K_{ftx}}{m} \\ a_9 = -\frac{K_{fty}}{m}, a_{10} = -\frac{K_{ftz}}{m}, b_0 = \frac{1}{I_x}, b_1 = \frac{1}{I_y}, b_2 = \frac{1}{I_z}, b_3 = \frac{1}{m} \end{cases}$$

$(K_{fax}, K_{fay}, K_{faz})$ represent the aerodynamic friction coefficients and $(K_{ftx}, K_{fty}, K_{ftz})$ are the translation drag coefficients, J_r denotes the rotor inertia, m and (I_x, I_y, I_z) are respectively the mass and the total inertia matrix of the quadrotor, finally u_5 and u_6 are two virtual inputs. The dynamic model of the quadrotor given in equation (6) has six outputs $(x, y, z, \phi, \theta, \psi)$ and only four independent inputs (u_1, u_2, u_3, u_4). Therefore, the quadrotor is an under-actuated system and hence it is not possible to control all the states simultaneously (Madani and Benallegue, 2007). A possible combination of controlled outputs can be (x, y, z, ψ) in order to track the desired positions and stabilise the roll and pitch angles (ϕ, θ) which introduce stable zero dynamics into the system. To deal with this problem, two virtual control inputs (u_5, u_6) are introduced in addition to the four control inputs of the quadrotor so that each output of the system will be controlled independently. The two virtual inputs are defined as

$$\begin{aligned} u_5 &= (\cos x_{11} \cos x_{31} \sin x_{21} + \sin x_{11} \sin x_{31}) \\ u_6 &= (\cos x_{11} \sin x_{21} \sin x_{31} - \sin x_{11} \cos x_{31}) \end{aligned} \tag{7}$$

Several techniques which consider unmodelled dynamics and aerodynamic interaction have been employed in various trajectories tracking controller designs for the quadrotor. Several recent papers related to UAV dealt with adaptive control-based onneural networks (NNs). In Emran and Najjaran (2017) an adaptive NN control of the quadrotor system with actuator constraints, however the authors did not consider the nonlinear function g_i to be fully known. RBF NNs have only one single hidden layer which can be easily tuned. This makes them more attractive than MLPNNs by referring to Haykin (2009) and Behera et al. (2010). A variety of NN adaptive control methods are proposed in the literature. However, in all these works, disturbances and parameter variations are not taken into consideration.

3 Proposed tracking control strategies for the quadrotor UAV

Two control methods are proposed in this work: an adaptive neural network-based H_∞ tracking control and an adaptive neural network-based H_∞ tracking controller with sliding mode to enhance system robustness and maintain boundedness. In addition, admissible laws are derived and the weights of RBF NNs are updated based on a Lyapunov function. It can be proven, for the two proposed methods, that the resulting closed-loop system is robustly stable and UUB. The adopted control strategy is based on two controllers one for the position andone for the attitude. The reference ofthe pitch and roll angles (ϕ_d, θ_d) are generated through the two virtual inputs u_5 and u_6, computed to follow the desired (x, y) movement, which are given by

$$\begin{cases} \phi_d = \arcsin\left(u_5 \sin\left(\psi_d\right) - u_6 \cos\left(\psi_d\right)\right) \\ \theta_d = \arcsin\left(\left(u_5 \cos\left(\psi_d\right) + u_6 \sin\left(\psi_d\right)\right)/\cos\left(\phi_d\right)\right) \end{cases} \tag{8}$$

The main objective is to design a controller for the miniature quadrotor UAV Figure 2 which exhibits robustness properties against unmodeled dynamics and parameter uncertainties, while ensuring that the position $x(t), y(t), z(t), \psi(t)$ tracks asymptotically the desired trajectory $x_d(t), y_d(t), z_d(t), \psi_d(t)$.

Figure 2 Scheme of the quadrotor (see online version for colours)

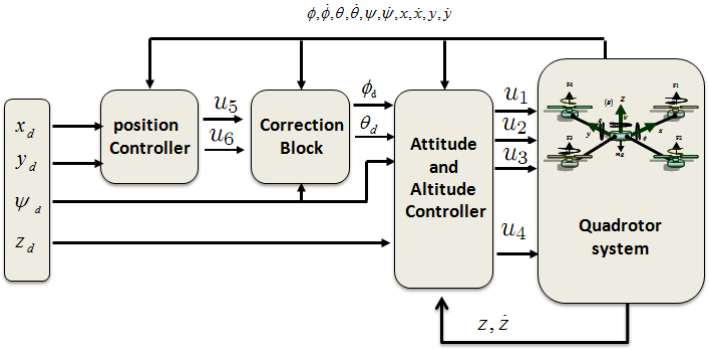

The state-space model of equation (1) can be rearranged as follow

$$\sum_i \begin{cases} \dot{x}_{i1} = x_{i2} \\ \dot{x}_{i2} = f_i(X) + g_i(X) u_i + d_i \ / i = (1, ..., 6) \\ y_i = x_{i1} \end{cases} \tag{9}$$

where $f_i(X)$ and $g_i(X)$ are nonlinear smooth functions and $u_i = [u_{1,...,}u_6]^T \in \Re^6$ is the control input vector, $y_i = [y_{1,...,}y_6]^T \in \Re^6$ is the output vector. d_i is an external bounded disturbance such that $|d_i| \leq \Delta_d$. Each of the two functions $f_i(X)$ and $g_i(X)$ can be written as the sum of two elements: Its nominal forms and an unknown bounded uncertainty.

$$\begin{cases} f_i(X) = f_{0i}(X) + \Delta f_i(X); |\Delta f_i(X)| \leq \Delta_f \\ g_i(X) = g_{0i}(X) + \Delta g_i(X); |\Delta g_i(X)| \leq \Delta_g \end{cases} / i = (1, ..., 6) \tag{10}$$

where Δ_f, Δ_g are positive constants, $\Delta f_i(X)$, $\Delta g_i(X)$ denote the uncertain terms and $f_i(X)$,$g_i(X)$ represent the nominal values. Substituting equation (10) into equation (9), yields

$$\sum_i \begin{cases} \dot{x}_{i1} = x_{i2} \\ \dot{x}_{i2} = f_{0i}(X) + g_{0i}(X) u_i + D_i \\ y_i = x_{i1} \end{cases} \tag{11}$$

where D_i is the sum of the external perturbation and the model uncertainty.

$$\begin{cases} D_i = \Delta f_i(X) + \Delta g_i(X) u_i + d_i \\ D_M = \Delta_f + \Delta_g u_M + \Delta_d; \ |u| \leq u_M \end{cases} \tag{12}$$

First express the parametric variations of the model coefficients

$$\begin{array}{lll} a_0 = a_0^0 + \Delta a_0; & a_5 = a_5^0 + \Delta a_5; & a_{10} = a_{10}^0 + \Delta a_{10} \\ a_1 = a_1^0 + \Delta a_1; & a_6 = a_6^0 + \Delta a_6; & b_0 = b_0^0 + \Delta b_0 \\ a_2 = a_2^0 + \Delta a_2; & a_7 = a_7^0 + \Delta a_7; & b_1 = b_1^0 + \Delta b_1 \\ a_3 = a_3^0 + \Delta a_3; & a_8 = a_8^0 + \Delta a_8; & b_2 = b_2^0 + \Delta b_2 \\ a_4 = a_4^0 + \Delta a_4; & a_9 = a_9^0 + \Delta a_9; & b_3 = b_3^0 + \Delta b_3 \\ g = g^0 + \Delta g & & \end{array} \tag{13}$$

The nominal model of the system is obtained as follows

$$\begin{array}{ll} f_{01}(X) = a_0^0 x_{22} x_{32} + a_1^0 \Omega_r x_{22} + a_2^0 {x_{12}}^2; & g_{01}(X) = b_0^0 \\ f_{02}(X) = a_3^0 x_{12} x_{32} + a_4^0 \Omega_r x_{12} + a_5^0 {x_{22}}^2; & g_{02}(X) = b_1^0 \\ f_{03}(X) = a_6^0 x_{12} x_{22} + a_7^0 {x_{32}}^2; & g_{03}(X) = b_2^0 \\ f_{04}(X) = a_{10}^0 x_{42} - g^0; & g_{04}(X) = b_3^0 \cos x_{11} \cos x_{21} \\ f_{05}(X) = a_8^0 x_{52}; & g_{05}(X) = b_3^0 u_4 \\ f_{06}(X) = a_9^0 x_{62}; & g_{06}(X) = b_3^0 u_4 \end{array} \tag{14}$$

with

$$y_i^{(2)} = \begin{pmatrix} y_1^{(2)} \\ \vdots \\ y_6^{(2)} \end{pmatrix}, f_{0i}(X) = \begin{pmatrix} f_{01}(X) \\ \vdots \\ f_{06}(X) \end{pmatrix}$$

$$g_{0i}(X) = \begin{pmatrix} g_{01}(X) & 0 & \cdots & 0 \\ 0 & g_{02}(X) & 0 & \vdots \\ \vdots & 0 & \ddots & 0 \\ 0 & \cdots & 0 & g_{06}(X) \end{pmatrix}$$

Let us define $D_1 ... D_6$ as follows

$$\begin{aligned} D_1 &= \underbrace{\Delta a_0 x_{22} x_{32} + \Delta a_1 \Omega_r x_{22} + \Delta a_2 x_{12}^2}_{\Delta f_1(X)} + \underbrace{\Delta b_0}_{\Delta g_1(X)} u_1 + d_1 \\ D_2 &= \underbrace{\Delta a_3 x_{12} x_{32} + \Delta a_4 \Omega_r x_{12} + \Delta a_5 x_{22}^2}_{\Delta f_2(X)} + \underbrace{\Delta b_1}_{\Delta g_2(X)} u_2 + d_2 \\ D_3 &= \underbrace{\Delta a_6 x_{12} x_{22} + \Delta a_7 x_{32}^2}_{\Delta f_3(X)} + \underbrace{\Delta b_2}_{\Delta g_3(X)} u_3 + d_3 \\ D_4 &= \underbrace{\Delta a_{10} x_{42} - \Delta g}_{\Delta f_4(X)} + \underbrace{\Delta b_3 \cos x_{11} \cos x_{21}}_{\Delta g_4(X)} u_4 + d_4 \\ D_5 &= \underbrace{\Delta a_8 x_{52}}_{\Delta f_5(X)} + \underbrace{\Delta b_3 u_4}_{\Delta g_5(X)} u_5 + d_5 \\ D_6 &= \underbrace{\Delta a_9 x_{62}}_{\Delta f_6(X)} + \underbrace{\Delta b_3 u_4}_{\Delta g_6(X)} u_6 + d_6 \end{aligned} \tag{15}$$

Assumption 2

1 The nonlinear system of equation (9) has a relative degree of n.

2 The control u_i appears linearly with respect to $y^{(n)}$, that is

$$y_i^{(n)} = f_{0i}(X) + g_{0i}(X)\, u_i + D_i / i = (1, ..., 6), n = 2 \tag{16}$$

However, in our case, these nonlinear functions are not known exactly. Therefore, the authors propose to use an adaptive neural model to approximate the nonlinear functions $f_{0i}(X)$ and $g_{0i}(X)$.

Assumption 3: The desired trajectory and its time derivatives are smooth and bounded.

Assumption 4: The sign of the nonlinear function $g_{0i}(X)$ is known and without loss of generality, the function is assumed to be positive definite and bounded $|g_{0i}(X)| \geq \underline{g}_{0i} > 0$, where $\underline{g}_{0i}$ is a positive constant.

Let us define the tracking error as

$$e_i = y_{di} - x_{i1}, \dot{e}_i = \dot{y}_{di} - x_{i2} \tag{17}$$

If the functions both $f_{0i}(X)$ and $g_{0i}(X)$ are assumed known and the disturbance vector then according to the feedback linearisable techniques (Isidori, 1989), the control law can be written as

$$u_i = (g_{0i}(X))^{-1} (v_i - f_{0i}(X)) / i = (1, ..., 6), n = 2 \tag{18}$$

Hence, $v_i(t) = y_{di}^{(n)}(t) + k_{i,n-1} e_i^{(n-1)}(t) + \cdots + k_{i,0} e_i(t)$, $E_i = \left[e_i, \dot{e}_i, ..., e_i^{(n-1)}\right]^T$ and $K_i = [k_{i,0}, ..., k_{i,n-1}]$ is the Hurwitz vector. Substituting equation (18) into equation (16) gives

$$y_i^{(n)} = y_{di}^{(n)} + K_i E_i \Rightarrow e_i^{(n)} + K_i E_i = 0 / i = (1, ..., 6), n = 2 \tag{19}$$

The aim of our study is to ensure output tracking of the desired trajectory, where $\lim_{t \to \infty} E_i(t) = 0$.

Since $f_{0i}(X)$ and $g_{0i}(X)$ are both unknown continuous functions, and the disturbance vector $D_i \neq 0$, so RBF NNs can be used to approximate these nonlinear functions (Long and Fei, 2008), Let's define

$$\begin{cases} f_{0i}(X) = W_{f_{0i}}^T h_{f_0 i}(X) + \zeta_{f_{0i}}(X) \\ g_{0i}(X) = W_{g_{0i}}^T h_{g_0 i}(X) + \zeta_{g_{0i}}(X) \end{cases} \tag{20}$$

where i = (1, 2, ..., 6), $X \in \Re^{12}$, $W_{f_{0i}}$ and $W_{g_{0i}}$ are vectors of adjustable weights and $\zeta_{f_{0i}}$, $\zeta_{g_{0i}}$ are approximation errors.

Assumption 5: The approximation errors $\zeta_{f_{0i}}$, $\zeta_{g_{0i}}$ are assumed to be bounded $|\zeta_{f_{0i}}| \leq \bar{\zeta}_{f_{0i}}, |\zeta_{g_{0i}}| \leq \bar{\zeta}_{g_{0i}}$ where and are known positive constants.

The Gaussian-type function can be expressed as

$$\begin{aligned} h_{f_0ij}(X) &= \exp\left[-(X-\eta_{f_0ij})^T(X-\eta_{f_0ij})\Big/\left(2\sigma^2{}_{f_0ij}\right)\right] \\ h_{g_0ij}(X) &= \exp\left[-(X-\eta_{g_0ij})^T(X-\eta_{g_0ij})\Big/\left(2\sigma^2{}_{g_0ij}\right)\right] \end{aligned} \tag{21}$$

$(\eta_{f_0ij}, \sigma_{f_0ij})$ and $(\eta_{g_0ij}, \sigma_{g_0ij})$ are the center and variance of the basis function respectively. The estimates of the unknown nonlinear RBF NNs functions $f_{0i}(X)$ and $g_{0i}(X)$ are given by

$$\begin{cases} \hat{f}_{0i}(X) = \hat{W}_{f_{f_{0i}}}^T h_{f_0i}(X) \\ \hat{g}_{0i}(X) = \hat{W}_{g_{0i}}^T h_{g_0i}(X) \end{cases} \tag{22}$$

Denoting the vectors of Gaussian basis function as

$$\begin{aligned} h_{f_0i}(X) &= [h_{f_0i1}(X), h_{f_0i2}(X), \ldots, h_{f_0iN}(X)] \\ h_{g_0i}(X) &= [h_{g_0i1}(X), h_{g_0i2}(X), \ldots, h_{g_0iq}(X)] \end{aligned} \tag{23}$$

where $h_{f_0i}(X): X \to \Re^N, h_{g_0i}(X): X \to \Re^q$, $\hat{W}_{f_{0i}}$ and $\hat{W}_{g_{0i}}$ are the estimate value of weights vector. Let us define the weights vector errors of RBF NNs as (Mellouli et al., 2018)

$$\begin{cases} \tilde{W}_{f_{0i}} = \hat{W}_{f_{0i}} - W_{f_{0i}}^* \\ \tilde{W}_{g_{0i}} = \hat{W}_{g_{0i}} - W_{g_{0i}}^* \end{cases} \tag{24}$$

where the optimal weights are given by

$$\begin{cases} W_{f_{0i}}^* = \underset{\hat{W}_{f_{oi}} \in S_f}{\arg\min} \left[\sup_{X \in \Re^n} \left| \hat{f}_{0i}(X) - f_{0i}(X) \right| \right] \\ W_{g_{0i}}^* = \underset{\hat{W}_{g_{0i}} \in S_g}{\arg\min} \left[\sup_{X \in \Re^n} \left| \hat{g}_{0i}(X) - g_{0i}(X) \right| \right] \end{cases} \tag{25}$$

S_f and S_g are known compact subsets.

$$\begin{aligned} S_f &= \left\{ \hat{W}_{f_{0i}} : \left\| \hat{W}_{f_{0i}} \right\| \leq M_{f_{0i}} \right\} \\ S_g &= \left\{ \hat{W}_{g_{0i}} : \left\| \hat{W}_{g_{0i}} \right\| \leq M_{g_{0i}} \right\} \end{aligned} \tag{26}$$

$M_{f_{0i}}$, $M_{g_{0i}}$ are positive constants. The compound disturbance of system (11) is defined as (Yu et al., 2010)

$$\omega_i(X) = \zeta_i(X) - D_i \tag{27}$$

where $\omega_i \in L_2[0, t_f]$, $\forall t_f \in [0, \infty)$ and ω_i is bounded, i.e.,$|\omega_i| \leq \bar{\omega}_i$.

The approximate errors are described by

$$\begin{aligned} \zeta_i &= \left(\hat{f}_{0i}\left(X, W_{f_{0i}}^*\right) - f_{0i}(X) \right) + \left(\hat{g}_{0i}\left(X, W_{g_{0i}}^*\right) - g_{0i}(X) \right) u_i \\ &= \left(\tilde{W}_{f_{0i}}^T h_{f_0i}(X) - \zeta_{f_{0i}}(X) \right) + \left(\tilde{W}_{g_{0i}}^T h_{g_0i}(X) - \zeta_{g_{0i}}(X) \right) u_i \end{aligned} \tag{28}$$

4 Design of the robust adaptive neural H_∞ tracking control (H_∞-ANC)

In this section, H_∞ is introduced to enhance the robustness of the control system and compensate the effects of the approximation errors ζ_i of RBF NNs and disturbances D_i. In the case where, $\omega_i \neq 0$ the following H_∞ tracking performance is required (Liu, 2008; Chen et al., 1997)

$$\begin{aligned}&\int_0^{t_f} E_i^T Q_i E_i dt \leq E_i^T(0) P_i E_i(0) + \gamma_{f_{0i}}^{-1} \tilde{W}_{f_{0i}}^T(0) \tilde{W}_{f_{0i}}(0) \\ &+\gamma_{g_{0i}}^{-1} \tilde{W}_{g_{0i}}^T(0) \tilde{W}_{g_{0i}}(0) + \rho_i^2 \int_0^{t_f} \omega_i^T \omega_i dt \\ &\forall t_f \in [0, \infty), \omega_i \in L_2[0, t_f]\end{aligned} \tag{29}$$

where Q_i are symmetrical positive semi-definite matrices, $\gamma_{g_{0i}} > 0$ and $\gamma_{f_{0i}} > 0$ are adaptive gains. $\|E_i\|_{Q_i}^2 = \int_0^{t_f} E_i^T Q_i E_i dt$, $\|\omega_i\|^2 = \int_0^{t_f} \omega_i^T \omega_i dt$ and ρ_i is a prescribed attenuation level.

Figure 3 Structure of H_∞-ANC control scheme (see online version for colours)

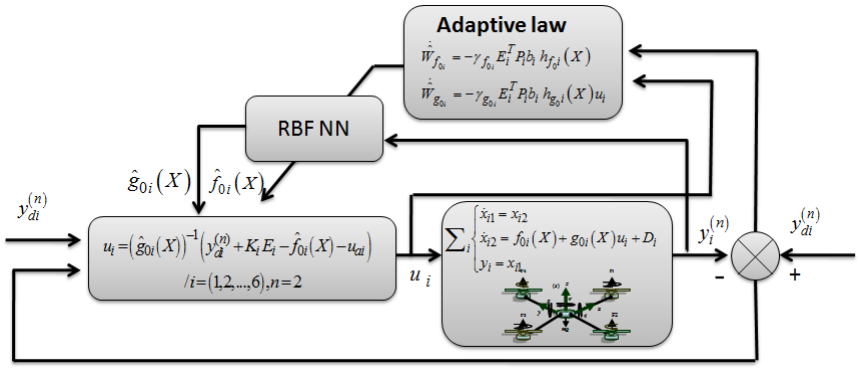

If $E_i(0) = 0$, $\tilde{W}_{f_{0i}}(0) = 0$, $\tilde{W}_{g_{0i}}(0) = 0$, the H_∞ performance can be rewritten as

$$\sup_{\omega_i \in L_2[0,t_f]} \frac{\|E_i\|_{Q_i}}{\|\omega_i\|} \leq \rho_i / i = 1, ..., 6 \tag{30}$$

The control law that ensures closed-loop system stability is obtained as

$$u_i = (\hat{g}_{0i}(X))^{-1} \left(y_{di}^{(n)} + K_i E_i - \hat{f}_{0i}(X) - u_{ai} \right) / i = 1, 2, ..., 6, n = 2 \tag{31}$$

u_{ai} is the control law associated with H_∞ robust control employed to compensate the neural network approximation error and the external disturbances.

Substituting equation (31) into equation (11), gives

$$e_i^{(n)} = -K_i E_i + \left(\hat{f}_{0i}(X) - f_{0i}(X) \right) + (\hat{g}_{0i}(X) - g_{0i}(X)) u_i + u_{ai} - D_i \tag{32}$$

From (32), (28) and (27) the output tracking error dynamic equation is obtained as

$$\begin{aligned}\dot{E}_i = &A_i E_i + b_i \left[\left(\hat{f}_{0i}(X) - \hat{f}_{0i}\left(X, W_{f_{0i}}^*\right) \right) \right. \\ &\left. + \left(\hat{g}_{0i}(X) - \hat{g}_{0i}\left(X, W_{g_{0i}}^*\right) \right) u_i + \omega_i + u_{ai} \right]\end{aligned} \tag{33}$$

with

$$A_i = \begin{bmatrix} 0 & 1 & 0 & \cdots 0 \\ 0 & 0 & 1 & \cdots 0 \\ \vdots & \vdots & \vdots & \ddots \vdots \\ -k_{i,0} & -k_{i,1} & -k_{i,2} & \cdots -k_{i,n-1} \end{bmatrix} \in \Re^{(n-1)\times(n-1)}, b_i = \begin{bmatrix} 0 \\ 0 \\ \vdots \\ 1 \end{bmatrix} \in \Re^{(n-1)}$$

The parameters $k_{i,0}, ..., k_{i,n-1}$ are chosen such that the A_i matrix is stable. Substituting equations (22) and (24) into equation (33) leads to

$$\begin{aligned} \dot{E}_i &= A_i E_i + b_i \left[\left(\left(\hat{W}_{f_{0i}} - W^*_{f_{0i}} \right)^T h_{f_0 i}(X) \right) \right. \\ &\quad \left. + \left(\left(\hat{W}_{g_{0i}} - W^*_{g_{0i}} \right)^T h_{g_0 i}(X) \right) u_i + \omega_i + u_{ai} \right] \\ &= A_i E_i + b_i \left[\left(\tilde{W}^T_{f_{0i}} h_{f_0 i}(X) \right) + \left(\tilde{W}^T_{g_{0i}} h_{g_0 i}(X) \right) u_i + \omega_i + u_{ai} \right] \\ &= A_i E_i + \chi_i + b_i \omega_i \end{aligned} \tag{34}$$

where $\chi_i = b_i \left[\left(\tilde{W}^T_{f_{0i}} h_{f_0 i}(X) \right) + \left(\tilde{W}^T_{g_{0i}} h_{g_0 i}(X) \right) u_i + u_{ai} \right]$.

Consider the following Lyapunov function

$$V_i = \frac{1}{2} E_i^T P_i E_i + \frac{1}{2\gamma_{f_{0i}}} \tilde{W}^T_{f_{0i}} \tilde{W}_{f_{0i}} + \frac{1}{2\gamma_{g_{0i}}} \tilde{W}^T_{g_{0i}} \tilde{W}_{g_{0i}} \tag{35}$$

The time derivative of V_i is

$$\dot{V}_i = \frac{1}{2} \dot{E}_i^T P_i E_i + \frac{1}{2} E_i^T P_i \dot{E}_i + \frac{1}{\gamma_{f_{0i}}} \tilde{W}^T_{f_{0i}} \dot{\tilde{W}}_{f_{0i}} + \frac{1}{\gamma_{g_{0i}}} \tilde{W}^T_{g_{0i}} \dot{\tilde{W}}_{g_{0i}} \tag{36}$$

By using the fact that $\dot{\tilde{W}}_{f_{0i}} = \dot{\hat{W}}_{f_{0i}}$ and $\dot{\tilde{W}}_{g_{0i}} = \dot{\hat{W}}_{g_{0i}}$ then

$$\begin{aligned} \dot{V}_i &= \tfrac{1}{2} \dot{E}_i^T P_i E_i + \tfrac{1}{2} E_i^T P_i \dot{E}_i + \tfrac{1}{\gamma_{f_{0i}}} \tilde{W}^T_{f_{0i}} \dot{\hat{W}}_{f_{0i}} + \tfrac{1}{\gamma_{g_{0i}}} \tilde{W}^T_{g_{0i}} \dot{\hat{W}}_{g_{0i}} \\ &= \tfrac{1}{2} \left[E_i^T \left(A_i^T P_i + P_i A_i \right) E_i \right] + \tfrac{1}{2} \left[E_i^T P_i b_i \omega_i + \omega_i^T b_i^T P_i E_i \right] \\ &\quad + E_i^T P_i \chi_i + \tfrac{1}{\gamma_{f_{0i}}} \tilde{W}^T_{f_{0i}} \dot{\hat{W}}_{f_{0i}} + \tfrac{1}{\gamma_{g_{0i}}} \tilde{W}^T_{g_{0i}} \dot{\hat{W}}_{g_{0i}} \end{aligned} \tag{37}$$

Substituting χ_i into equation (37) gives

$$\begin{aligned} \dot{V}_i &= \tfrac{1}{2} \left[E_i^T \left(A_i^T P_i + P_i A_i - 2\mu_i^{-1} P_i b_i b_i^T P \right) E_i \right] \\ &\quad + \tfrac{1}{\gamma_{f_{0i}}} \tilde{W}^T_{f_{0i}} \left[\gamma_{f_{0i}} E_i^T P_i b_i h_{f_0 i}(X) + \dot{\hat{W}}_{f_{0i}} \right] \\ &\quad + \tfrac{1}{\gamma_{g_{0i}}} \tilde{W}^T_{g_{0i}} \left[\gamma_{g_{0i}} E_i^T P_i b_i h_{g_0 i}(X) u_i + \dot{\hat{W}}_{g_{0i}} \right] \\ &\quad + \tfrac{1}{2} \left[E_i^T P_i b_i \omega_i + \omega_i^T b_i^T P_i E_i \right] \end{aligned} \tag{38}$$

To ensure that the control objectives are achieved, the following adaptation laws are chosen

$$\begin{aligned} \dot{\hat{W}}_{f_{0i}} &= -\gamma_{f_{0i}} E_i^T P_i b_i h_{f_0 i}(X) \\ \dot{\hat{W}}_{g_{0i}} &= -\gamma_{g_{0i}} E_i^T P_i b_i h_{g_0 i}(X) u_i \end{aligned} \tag{39}$$

Moreover, choosing $u_{ai} = -\mu_i^{-1} b_i^T P_i E_i$, then

$$\begin{aligned} \dot{V}_i &= \tfrac{1}{2}\left[E_i^T\left(A_i^T P_i + P_i A_i - 2\mu_i^{-1} P_i b_i b_i^T P\right) E_i\right] \\ &\quad + \tfrac{1}{2}\left[E_i^T P_i b_i \omega_i + \omega_i^T b_i^T P_i E_i\right] \end{aligned} \tag{40}$$

Thus, for any given matrix $Q_i = Q_i^T > 0$ there exists a matrix $P_i = P_i^T > 0$ which is a unique solution of the following Riccati equation

$$A_i^T P_i + P_i A_i - (\frac{2}{\mu_i} - \frac{1}{\rho_i^2}) P_i b_i b_i^T P_i = -Q_i \tag{41}$$

Remark 1: Equation (41) has a positive semi-definite and symmetric solution P_i if and only if $2\rho_i^2 \geq \mu_i$ (Anderson and Moore, 1993). Schur complement formula is used to transform equation (41) into the equivalent linear matrix inequalities (LMI) which is defined by Horn and Johnson (1985) and Long and Fei (2008).

$$\begin{pmatrix} A_i^T P_i + P_i A_i + Q_i & (\sqrt{\rho_i^{-2} - 2\mu_i^{-1}}) P_i b_i \\ (\sqrt{\rho_i^{-2} - 2\mu_i^{-1}}) b_i^T P_i & -I \end{pmatrix} < 0, \qquad P_i > 0 \tag{42}$$

From equations (41) and (40)

$$\begin{aligned} \dot{V}_i &= -\tfrac{1}{2} E_i^T Q_i E_i - \tfrac{1}{2\rho_i^2} E_i^T P_i b_i b_i^T P_i E_i + \tfrac{1}{2}\left[E_i^T P_i b_i \omega_i + \omega_i^T b_i^T P_i E_i\right] \\ &= -\tfrac{1}{2} E_i^T Q_i E_i - \tfrac{1}{2}\left(\tfrac{1}{\rho_i} b_i^T P_i E_i - \rho_i \omega_i\right)^T \left(\tfrac{1}{\rho_i} b_i^T P_i E_i - \rho_i \omega_i\right) \\ &\quad + \tfrac{1}{2}\rho_i^2 \omega_i^T \omega_i \leq -\tfrac{1}{2} E_i^T Q_i E_i + \tfrac{1}{2}\rho_i^2 \omega_i^T \omega_i \leq -\tfrac{1}{2}\left\|E_i\right\|_{Q_i}^2 + \tfrac{1}{2}\rho_i^2 \|\omega_i\|^2 \end{aligned} \tag{43}$$

Because $V_i(0)$ is bounded, and $V_i(t_f) \geq 0$ the following result is obtained

$$\begin{aligned} \tfrac{1}{2}\int_0^{t_f} E_i^T Q_i E_i dt &\leq V_i(0) + \tfrac{1}{2}\rho_i^2 \int_0^{t_f} \omega_i^T \omega_i dt \\ &= \tfrac{1}{2} E_i^T(0) P_i E_i(0) + \tfrac{1}{2\gamma_{f_{0i}}} \tilde{W}_{f_{0i}}^T(0) \tilde{W}_{f_{0i}}(0) \\ &\quad + \tfrac{1}{2\gamma_{g_{0i}}} \tilde{W}_{g_{0i}}^T(0) \tilde{W}_{g_{0i}}(0) + \tfrac{1}{2}\rho_i^2 \int_0^{t_f} \omega_i^T \omega_i dt \end{aligned} \tag{44}$$

If $V_i(0) = 0$, then equation (44) becomes

$$\sup_{\omega_i \in L_2[0,t_f]} \frac{\|E_i\|_{Q_i}}{\|\omega_i\|} \leq \rho_i$$

Which is equivalent to equation (29). It can be concluded that as Therefore, the tracking errors and their derivatives converge asymptotically to zero, hence the controller is strongly robust with respect to the compound disturbance. To ensure that the weights of RBF NNs are bounded, from Assumption 3, the neural adaptive laws for updating the weights in terms of the projection approach (Wang, 1989) are defined as

$$\dot{\hat{W}}_{f_{0i}} = \begin{cases} -\gamma_{f_{0i}} E_i^T P_i b_i h_{f_0 i}(X) & \text{if } \left\|\hat{W}_{f_{0i}}\right\| < M_{f_{0i}} \\ \text{or } \left(\left\|\hat{W}_{f_{0i}}\right\| = M_{f_{0i}} \text{ and } \right. & \\ \left. E_i^T P_i b_i \hat{W}_{f_{0i}}^T h_{f_0 i}(X) \geq 0 \right) & \\ p_{f_{0i}} \left[-\gamma_{f_{0i}} E_i^T P_i b_i h_{f_0 i}(X) \right] & \text{if } \left\|\hat{W}_{f_{0i}}\right\| = M_{f_{0i}} \\ \text{and } \left(E_i^T P_i b_i \hat{W}_{f_{0i}}^T h_{f_0 i}(X) < 0 \right) & \end{cases} \tag{45}$$

$$\dot{\hat{W}}_{g_{0i}} = \begin{cases} -\gamma_{g_{0i}} E_i^T P_i b_i h_{g_0 i}(X) u_i & \text{if } \left\|\hat{W}_{g_{0i}}\right\| < M_{g_{0i}} \\ \text{or } \left(\left\|\hat{W}_{g_{0i}}\right\| = M_{g_{0i}} \text{ and } \right. & \\ \left. E_i^T P_i b_i \hat{W}_{g_{0i}}^T h_{g_0 i}(X) u_i \geq 0 \right) & \\ p_{g_{0i}} \left[-\gamma_{g_{0i}} E_i^T P_i b_i h_{g_0 i}(X) u_i \right] & \text{if } \left\|\hat{W}_{g_{0i}}\right\| = M_{g_{0i}} \\ \text{and } \left(E_i^T P_i b_i \hat{W}_{g_{0i}}^T h_{g_0 i}(X) u_i < 0 \right) & \end{cases} \tag{46}$$

where

$$p_{f_{0i}} \left[-\gamma_{f_{0i}} E_i^T P_i b_i h_{f_0 i}(X) \right] = -\gamma_{f_{0i}} E_i^T P_i b_i h_{f_0 i}(X) + \frac{\gamma_{f_{0i}} E_i^T P_i b_i \hat{W}_{f_{0i}} \hat{W}_{f_{0i}}^T h_{f_0 i}(X)}{\left\|\hat{W}_{f_{0i}}\right\|^2} \tag{47}$$

$$p_{g_{0i}} \left[-\gamma_{g_{0i}} E_i^T P_i b_i h_{g_0 i}(X) u_i \right] = -\gamma_{g_{0i}} E_i^T P_i b_i h_{g_0 i}(X) u_i + \frac{\gamma_{g_{0i}} E_i^T P_i b_i \hat{W}_{g_{0i}} \hat{W}_{g_{0i}}^T h_{g_0 i}(X) u_i}{\left\|\hat{W}_{g_{0i}}\right\|^2} \tag{48}$$

To eliminate the effects of uncertain dynamics and external disturbances so that the output tracking error asymptotically converges to zero, a robust neural sliding mode tracking control system, which comprises an adaptive RBF NNs controller is developed in the following section.

5 Design of the robust adaptive H_∞ neural SMC (H_∞-ANSMC)

SMC is an effective robust control approach for a class of nonlinear systems with uncertainties defined in compact sets (Devika and Thomas, 2018). When the mathematical models are known, such a control is used directly to track the reference signals (Sira-Ramírez, 2015; Beyhan and Ali, 2009). H_∞ tracking control design method and adaptive neural SMC technique are combined to form the H_∞-ANSMC

controller for the quadrotor UAV. The proposed method not only is robust against approximate errors, disturbances and unmodelled dynamics, but also guarantees a desired H_∞ tracking performance for the overall system. Moreover, control chattering inherent in conventional SMC can be significantly reduced. The proposed H_∞ adaptive neural-based sliding mode tracking controller is depicted in Figure 4.

Figure 4 H_∞-ANSMC controller for i^{th} sub-system (see online version for colours)

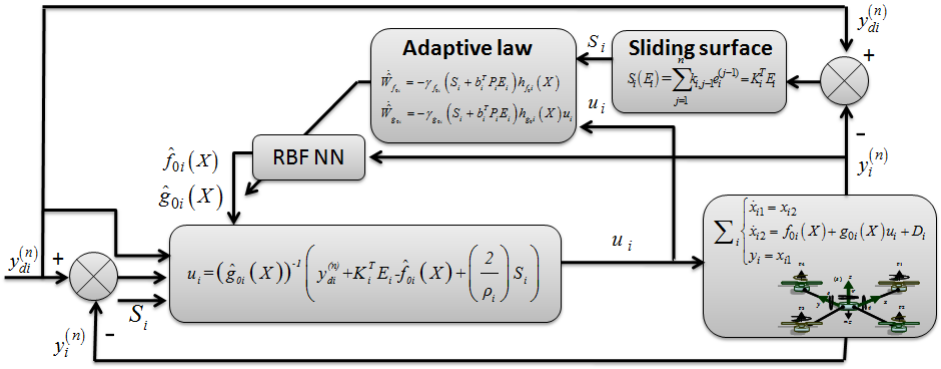

The H_∞ tracking performance for the overall system satisfies the following relationship

$$\begin{aligned}&\int_0^{t_f} E_i^T Q_i E_i dt \le S_i^2(0) + E_i^T(0) P_i E_i(0) + \gamma_{f_{0i}}^{-1} \tilde{W}_{f_{0i}}^T(0) \tilde{W}_{f_{0i}}(0) \\ &+\gamma_{g_{0i}}^{-1} \tilde{W}_{g_{0i}}^T(0) \tilde{W}_{g_{0i}}(0) + \rho_i^2 \int_0^{t_f} \omega_i^T \omega_i dt \\ &\forall t_f \in [0,\infty), \omega_i \in L_2[0,t_f]\end{aligned} \tag{49}$$

Consider the uncertain nonlinear systems (11), defining the sliding surface of the control systems as

$$\begin{aligned}S_i(E_i) &= k_{i,0} e_i + k_{i,1} \dot{e}_i + .. + k_{i,n-1} e_i^{(n-1)} + e_i^{(n-1)} \\ &= \sum_{j=1}^{n} k_{i,j-1} e_i^{(j-1)} = K_i^T E_i \quad /i = (1,2,...,6), n = 2\end{aligned} \tag{50}$$

where $E_i = \left[e_i, \dot{e}_i, ..., e_i^{(n-1)}\right]^T$, $K_i = [k_{i,0}, ..., k_{i,n-1}]^T$ is satisfied with the Hurwitz stability condition.

If $f_{0i}(X)$ and $g_{0i}(X)$ are exactly known, the control objective could be achieved by the following control law (Slotine and Li, 1991)

$$u_i = u_{eq_i} + u_{d_i} \tag{51}$$

where u_{eq_i} is the equivalent control law and u_{d_i} is the switching control law defined as

$$u_{d_i} = -\varepsilon_i \text{sgn}(S_i) \tag{52}$$

The term ε_i is a positive constant satisfying $\varepsilon_i > \frac{\Delta_{D_i}}{g_{0i}(X)}$. Where Δ_{D_i} denotes the bound of $D_i(t)$, that is $D_i(t) \le \Delta_{D_i}$ and

$$\text{sgn}(S_i) \begin{cases} 1 & \text{if} \quad S_i > 0 \\ 0 & \text{if} \quad S_i = 0 \\ -1 & \text{if} \quad S_i < 0 \end{cases}$$

However, if both functions $f_{0i}(X)$ and $g_{0i}(X)$ in equation (11) were unknown, then the control law (51) would be generally inapplicable. This explains the use of neural networks models to approximate these unknown nonlinear dynamics. On the basis of the certainty equivalent control approach (Slotine and Li, 1991), the control law (51) can be replaced with the following control law

$$u_i = \hat{u}_{eq_i} + \hat{u}_{d_i} \tag{53}$$

Based on the linearisation feedback technique, the equivalent control law in equation (53) is defined as

$$\hat{u}_{eq_i} = \left(\hat{g}_{0i}(X)\right)^{-1} \left(y_{di}^{(n)} + \underbrace{\sum_{j=1}^{n} k_{i,j-1} e_i^{(j-1)}}_{K_i E_i} - \hat{f}_{0i}(X) \right) \quad i = (1, ..., 6), n = 2 \tag{54}$$

and

$$\hat{u}_{d_i} = -\hat{\varepsilon}_i \text{sgn}(S_i) \tag{55}$$

where $\hat{\varepsilon}_i$, is a positive scalar. The rest of this section will focus on the design of the control and the adaptive laws $\dot{\hat{W}}_{f_{0i}}$ and $\dot{\hat{W}}_{g_{0i}}$ so that H_∞ tracking performance in equation (49) is achieved. Let $\hat{\varepsilon}_i = \left(\hat{g}_{0i}(X)\right)^{-1} (2/\rho_i) |S_i|$. Substituting this into equation (55), gives

$$\hat{u}_{d_i} = -\hat{\varepsilon}_i \text{sgn}(S_i) = -\left(\hat{g}_{0i}(X)\right)^{-1} \left(\frac{2}{\rho_i}\right) S_i \tag{56}$$

The chattering effect of the control input is substantially reduced with this method because the term $\hat{\varepsilon}_i \text{sgn}(S_i)$ related to the control chattering is replaced by a much smoother term $\left(\hat{g}_{0i}(X)\right)^{-1} (2/\rho_i) S_i$ in the derived control law. Therefore the control law u_i given by equation (53) can be rewritten as follows

$$u_i = \left(\hat{g}_{0i}(X)\right)^{-1} \left(y_{di}^{(n)} + K_i^T E_i - \hat{f}_{0i}(X) + \left(\frac{2}{\rho_i}\right) S_i \right) \tag{57}$$

Substituting equation (53) into equation (11) and from equation (19) and after a few transformations, the following dynamic error equation is obtained as

$$\begin{aligned} e_i^{(n)} = & -K_i E_i + \left(\hat{f}_{0i}(X) - f_{0i}(X)\right) + \left(\hat{g}_{0i}(X) - g_{0i}(X)\right) \\ & - \hat{\varepsilon}_i \hat{g}_{0i}(X) \text{sgn}(S_i) - D_i \end{aligned} \tag{58}$$

or

$$\begin{aligned} \dot{E}_i = & A_i E_i + b_i \left[\left(\hat{f}_{0i}(X) - f_{0i}(X)\right) + \left(\hat{g}_{0i}(X) - g_{0i}(X)\right) u_i \right] \\ & + b_i \left[-\hat{\varepsilon}_i \hat{g}_{0i}(X) \text{sgn}(S_i) - D_i \right] \end{aligned} \tag{59}$$

Substituting equations (22) and (24) into equation (59) gives

$$\begin{aligned}\dot{E}_i=&A_iE_i+b_i\left[\left(\hat{f}_{0i}\left(X\right)-f_{0i}\left(X\right)+\hat{f}_{0i}\left(X,W_{f_{0i}}^{*}\right)-\hat{f}_{0i}\left(X,W_{f_{0i}}^{*}\right)\right)\right.\\&\left.+\left(\hat{g}_{0i}\left(X\right)-g_{0i}\left(X\right)+\hat{g}_{0i}\left(X,W_{g_{0i}}^{*}\right)-\hat{g}_{0i}\left(X,W_{g_{0i}}^{*}\right)\right)\ u_i\right]\\&+b_i\left[-\hat{\varepsilon}_i\hat{g}_{0i}\left(X\right)\operatorname{sgn}\left(S_i\right)-D_i\right]\\=&A_iE_i+b_i\left[\left(\tilde{W}_{f_{0i}}^{T}h_{f_{0i}}\left(X\right)\right)+\left(\tilde{W}_{g_{0i}}^{T}h_{g_{0}i}\left(X\right)\right)u_i+\omega_i-\left(\tfrac{2}{\rho_i}\right)S_i\right]\end{aligned}\tag{60}$$

By calculating the time derivative, the sliding model dynamic equation is obtained as follows

$$\begin{aligned}\dot{S}_i&=K_i\dot{E}_i=y_{di}^{(n)}+K_i^TE_i-y_i^{(n)}\\&=\left(\tilde{W}_{f_{0i}}^{T}h_{f_{0}i}\left(X\right)\right)+\left(\tilde{W}_{g_{0i}}^{T}h_{g_{0}i}\left(X\right)\right)u_i+\omega_i-\left(\tfrac{2}{\rho_i}\right)S_i\end{aligned}\tag{61}$$

Define the Lyapunov function as

$$\begin{aligned}V_i=&\tfrac{1}{2}S_i^2+\tfrac{1}{2}E_i^TP_iE_i+\tfrac{1}{2\gamma_{f_{0i}}}\tilde{W}_{f_{0i}}^{T}\tilde{W}_{f_{0i}}\\&+\tfrac{1}{2\gamma_{g_{0i}}}\tilde{W}_{g_{0i}}^{T}\tilde{W}_{g_{0i}}\qquad\qquad i=(1,...,6),n=2\end{aligned}\tag{62}$$

where $\gamma_{f_{0i}}>0$, $\gamma_{g_{0i}}>0$ denote the adaptive gains. Using equation (60), the time derivative of V_i, is obtained as

$$\begin{aligned}\dot{V}_i&=S_i\dot{S}_i+\tfrac{1}{2}\dot{E}_i^TP_iE_i+\tfrac{1}{2}E_i^TP_i\dot{E}_i+\tfrac{1}{\gamma_{f_{0i}}}\tilde{W}_{f_{0i}}^{T}\dot{\tilde{W}}_{f_{0i}}+\tfrac{1}{\gamma_{g_{0i}}}\tilde{W}_{g_{0i}}^{T}\dot{\tilde{W}}_{g_{0i}}\\&=S_i\omega_i+\left(S_i+b_i^TP_iE_i\right)\left[\tilde{W}_{f_{0i}}^{T}h_{f_{0}i}\left(X\right)+\tilde{W}_{g_{0i}}^{T}h_{g_{0}i}\left(X\right)u_i\right]\\&+\tfrac{1}{2}\left[E_i^T\left(A_i^TP_i+P_iA_i\right)E_i\right]+\tfrac{1}{2}\left[E_i^TP_ib_i\omega_i+\omega_i^Tb_i^TP_iE_i\right]\\&-\left(\tfrac{2}{\rho_i}\right)S_i^2-\left(\tfrac{2}{\rho_i}\right)S_ib_i^TP_iE_i+\tfrac{1}{\gamma_{f_{0i}}}\tilde{W}_{f_{0i}}^{T}\dot{\tilde{W}}_{f_{0i}}+\tfrac{1}{\gamma_{g_{0i}}}\tilde{W}_{g_{0i}}^{T}\dot{\tilde{W}}_{g_{0i}}\end{aligned}\tag{63}$$

Again using the fact that $\dot{\tilde{W}}_{f_{0i}}=\dot{\hat{W}}_{f_{0i}}$ and $\dot{\tilde{W}}_{g_{0i}}=\dot{\hat{W}}_{g_{0i}}$ equation (63) becomes

$$\begin{aligned}\dot{V}_i&=S_i\omega_i+\left(S_i+b_i^TP_iE_i\right)\left[\tilde{W}_{f_{0i}}^{T}h_{f_{0}i}\left(X\right)+\tilde{W}_{g_{0i}}^{T}h_{g_{0}i}\left(X\right)u_i\right]\\&=S_i\omega_i-\left(\tfrac{2}{\rho_i}\right)S_ib_i^TP_iE_i+\tfrac{1}{\gamma_{f_{0i}}}\tilde{W}_{f_{0i}}^{T}\left[\gamma_{f_{0i}}\left(S_i+b_i^TP_iE_i\right)h_{f_{0}i}\left(X\right)\right.\\&\left.+\dot{\hat{W}}_{f_{0i}}\right]+\tfrac{1}{\gamma_{g_{0i}}}\tilde{W}_{g_{0i}}^{T}\left[\gamma_{g_{0i}}\left(S_i+b_i^TP_iE_i\right)h_{g_{0}i}\left(X\right)u_i+\dot{\hat{W}}_{g_{0i}}\right]\\&+\tfrac{1}{2}\omega_ib_i^TP_iE_i-\left(\tfrac{2}{\rho_i}\right)S_i^2+\tfrac{1}{2}\left[E_i^T\left(A_i^TP_i+P_iA_i\right)E_i\right]\end{aligned}\tag{64}$$

To guarantee that the weights of RBF NNs remain bounded the following weights update laws are used

$$\begin{aligned}\dot{\hat{W}}_{f_{0i}}&=-\gamma_{f_{0i}}\left(S_i+b_i^TP_iE_i\right)h_{f_{0}i}\left(X\right)\\\dot{\hat{W}}_{g_{0i}}&=-\gamma_{g_{0i}}\left(S_i+b_i^TP_iE_i\right)h_{g_{0}i}\left(X\right)u_i\end{aligned}\tag{65}$$

Then

$$\begin{aligned}\dot{V}_i&\leq S_i\omega_i-\left(\tfrac{2}{\rho_i}\right)S_ib_i^TP_iE_i+\omega_ib_i^TP_iE_i-\left(\tfrac{2}{\rho_i}\right)S_i^2\\&+\tfrac{1}{2}\left[E_i^T\left(A_i^TP_i+P_iA_i\right)E_i\right]\\&\leq\tfrac{1}{2}\left[E_i^T\left(A_i^TP_i+P_iA_i+\tfrac{4}{\rho_i}P_ib_ib_i^TP_i\right)E_i\right]+\tfrac{1}{2}\rho_i\omega_i^2\\&\leq-\tfrac{1}{2\rho_i}E_i^TQ_iE_i+\tfrac{1}{2}\rho_i\omega_i^2\end{aligned}\tag{66}$$

Consider the nonlinear system given by equation (11) with unknown bounded smooth functions $f_{0i}(X)$ and $g_{0i}(X)$, which are approximated by $\hat{f}_{0i}(X)$ and $\hat{g}_{0i}(X)$ respectively and suppose that, for any given $\rho_i > 0$, Q_i is a given symmetric positive definite weighting matrix.

Let $P_i = P_i^T$ be the solution of the following quadratic matrix inequality

$$A_i^T P_i + P_i A_i + \frac{4}{\rho_i} P_i b_i b_i^T P_i + \frac{Q_i}{\rho_i} \leq 0 \tag{67}$$

Note that the quadratic matrix inequality in equation (67) can be transformed into a certain form of LMI by referring to Horn and Johnson (1985) and Anderson and Moore (1993). That is, by the Schur complements, equation (67) is equivalent to

$$\begin{pmatrix} A_i^T P_i + P_i A_i + \frac{Q_i}{\rho_i} & \left(2\left(\sqrt{\rho_i}\right)^{-1}\right) P_i b_i \\ \left(2\left(\sqrt{\rho_i}\right)^{-1}\right) b_i^T P_i & -I \end{pmatrix} < 0, \quad P_i > 0 \tag{68}$$

Integrating the above inequality from 0 to t_f yields

$$\int_0^{t_f} \dot{V}_i \leq -\frac{1}{2\rho_i} \int_0^{t_f} E_i^T Q_i E_i dt + \frac{\rho_i}{2} \int_0^{t_f} \omega_i^2 dt \tag{69}$$

Thus

$$\frac{1}{2} \int_0^{t_f} E_i^T Q_i E_i dt \leq \rho_i V_i(0) - \rho_i V_i(t_f) + \frac{\rho_i^2}{2} \int_0^{t_f} \omega_i^2 dt \tag{70}$$

As $\rho_i > 0$ and $V_i \geq 0$, using equations (62) and (70) can be rewritten as

$$\begin{aligned} \tfrac{1}{2} \int_0^{t_f} E_i^T Q_i E_i dt &\leq V_i(0) + \tfrac{1}{2}\rho_i^2 \int_0^{t_f} \omega_i^2 dt \\ &= \tfrac{1}{2} S^2(0) + \tfrac{1}{2} E_i^T(0) P_i E_i(0) + \tfrac{1}{2\gamma_{f_{0i}}} \tilde{W}_{f_{0i}}^T(0) \tilde{W}_{f_{0i}}(0) \\ &+ \tfrac{1}{2\gamma_{g_{0i}}} \tilde{W}_{g_{0i}}^T(0) \tilde{W}_{g_{0i}}(0) + \tfrac{1}{2}\rho_i^2 \int_0^{t_f} \omega_i^T \omega_i dt \end{aligned} \tag{71}$$

Remark 2: If ω_i is square integrable (i.e., $\int_0^\infty \omega_i^2 = \omega_i^T \omega_i dt < \infty$), then $\lim_{t\to\infty} |E_i(t)| = 0$. Hence the H_∞ tracking performance in equation (49) is achieved.

By using the projection algorithm, the adaptive laws must be modified as

$$\dot{\hat{W}}_{f_{0i}} = \begin{cases} -\gamma_{f_{0i}} \left(S_i + b_i^T P_i E_i\right) h_{f_0 i}(X) & \text{if } \left\|\hat{W}_{f_{0i}}\right\| < M_{f_{0i}} \\ \text{or } \left(\left\|\hat{W}_{f_{0i}}\right\| = M_{f_{0i}} \text{ and} \right. & \\ \left. \left(S_i + b_i^T P_i E_i\right) h_{f_0 i}(X) \geq 0 \right) & \\ p_{f_{0i}} \left[-\gamma_{f_{0i}} \left(S_i + b_i^T P_i E_i\right) h_{f_0 i}(X)\right] & \text{if } \left\|\hat{W}_{f_{0i}}\right\| = M_{f_{0i}} \\ \text{and } \left(\left(S_i + b_i^T P_i E_i\right) h_{f_0 i}(X) < 0 \right) & \end{cases} \tag{72}$$

$$\dot{\hat{W}}_{g_{0i}} = \begin{cases} -\gamma_{g_{0i}} \left(S_i + b_i^T P_i E_i\right) h_{g_0 i}\left(X\right) u_i & \text{if } \left\|\hat{W}_{g_{0i}}\right\| < M_{g_{0i}} \\ \text{or } \left(\left\|\hat{W}_{g_{0i}}\right\| = M_{g_{0i}} \text{ and } \right. & \\ \left. \left(S_i + b_i^T P_i E_i\right) h_{g_0 i}\left(X\right) u_i \geq 0\right) & \\ p_{g_{0i}}\left[-\gamma_{g_{0i}} \left(S_i + b_i^T P_i E_i\right) h_{g_0 i}\left(X\right) u_i\right] & \text{if } \left\|\hat{W}_{g_{0i}}\right\| = M_{g_{0i}} \\ \text{and } \left(\left(S_i + b_i^T P_i E_i\right) h_{g_0 i}\left(X\right) u_i < 0\right) & \end{cases} \tag{73}$$

where

$$p_{f_{0i}}\left[-\gamma_{f_{0i}} \left(S_i + b_i^T P_i E_i\right) h_{f_0 i}\left(X\right)\right] = -\gamma_{f_{0i}} \left(S_i + b_i^T P_i E_i\right) h_{f_0 i}\left(X\right) + \frac{\gamma_{f_{0i}}\left(S_i + b_i^T P_i E_i\right)\hat{W}_{f_{0i}} \hat{W}_{f_{0i}}^T h_{f_0 i}(X)}{\left\|\hat{W}_{f_{0i}}\right\|^2} \tag{74}$$

$$p_{g_{0i}}\left[-\gamma_{g_{0i}} \left(S_i + b_i^T P_i E_i\right) h_{g_0 i}\left(X\right) u_i\right] = -\gamma_{g_{0i}} \left(S_i + b_i^T P_i E_i\right) h_{g_0 i}\left(X\right) u_i + \frac{\gamma_{g_{0i}}\left(S_i + b_i^T P_i E_i\right)\hat{W}_{g_{0i}} \hat{W}_{g_{0i}}^T h_{g_0 i}(X) u_i}{\left\|\hat{W}_{g_{0i}}\right\|^2} \tag{75}$$

From the above discussion, a design procedure for the H_∞-ANSMC is performed in the following three steps:

Step 1 Construct the RBF NNs models to estimate the unknown nonlinear functions $f_{0i}\left(X\right)$ and $g_{0i}\left(X\right)$ in equation (22), and specify a suitable sliding surface $S_i\left(E_i\right) = K_i^T E_i = 0$ as given in equation (50).

Step 2 Specify Q_i and a prescribed attenuation level ρ_i. Then, solve the quadratic matrix inequality given by equation (67) to obtain P_i.

Step 3 Obtain the control law (57) for the nonlinear system given by equation (11) and adjust $\hat{W}_{f_{0i}}$ and $\hat{W}_{g_{0i}}$ using the adaptive laws given by equations (72) and (73).

6 Simulation results and discussion

In order to validate and test the performance of the designed H_∞-ANSMC control strategy, a series of simulations are presented. Furthermore, the proposed controller is compared with the adaptive neural networks-based H_∞ tracking control approach taking into account wind disturbance and parameter uncertainties. The wind is represented as the extra acceleration and affects all x, y and z axis, which is depicted in Figure 5. The

wind disturbance has a maximum acceleration of about 1.8 m/s^2. The total simulation time is 140 s. With $d_i(t) = \bar{d}_i(t) + N$, N: Gaussian white noise 24 dB

$$\bar{d}_i(t) = \begin{cases} 0 & \text{if} \quad 0 \le t \le t_1 \\ 0.8\sin\left(\frac{\pi(t-t_1)}{31}\right) + 0.4\sin\left(\frac{\pi(t-t_1)}{7}\right) & \\ +0.08\sin\left(\frac{\pi(t-t_1)}{2}\right) + 0.056\sin\left(\frac{24\pi(t-t_1)}{11}\right) & \text{if} \quad t_1 < t \le t_2 \\ 0 & \text{if} \quad t_2 < t \le t_3 \\ 1.37\sin\left(\frac{\pi(t-t_3)}{55}\right) + 0.15\sin\left(\frac{\pi(t-t_3)}{2}\right) & \\ +0.225\sin\left(\frac{\pi(t-t_3)}{5}\right) + 0.105\sin\left(\frac{24\pi(t-t_3)}{11}\right) & \text{if} \quad t_3 < t \le t_4 \\ 0 & \text{if} \quad t_4 \le t \le t_5 \end{cases}$$

t_1 = 30 s, t_2 = 57 s, t_3 = 70 s, t_4 = 124 s, t_5 = 140 s.

Figure 5 Wind disturbance profile

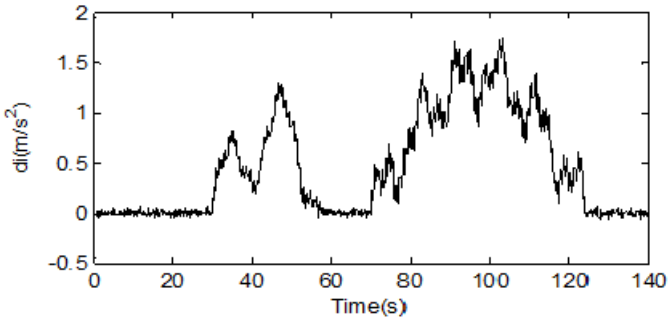

The uncertainty in the model parameters has been increased by 50% for $(\Delta a_0 ... \Delta a_{10})$ and 40% for $(\Delta b_0 ... \Delta b_3)$, the gravity was varied by 10%. The parameters values of the quadrotor model used in the simulation are based on the real platform described in Bouadi et al. (2007). The control objective is that the actual output $y_i = x_{i1}$ follows the desired trajectories

$$x_d(t) = \begin{cases} 0 & \text{if} \quad 0 \le t \le t_1 \\ -2\cos\left(\frac{(\pi/2)(t-t_1)^5}{(t-t_1)^5+(t_2-t)^5}\right) + 2 & \text{if} \quad t_1 \le t < t_2 \\ \frac{10(t-t_2)^5}{\left((t-t_2)^5+(t_3-t)^5\right)+2} & \text{if} \quad t_2 \le t < t_3 \\ 2\sin\left(\frac{(\pi/2)(t-t_3)^5}{(t-t_3)^5+((3t_5/5)-t)^5}\right) + 12 & \text{if} \quad t_3 \le t \le t_5 \end{cases}$$

$$y_d(t) = \begin{cases} 0 & \text{if} \quad 0 \le t \le t_3 \\ -2\cos\left(\frac{(\pi/2)(t-t_3)^5}{(t-t_3)^5+(t_4-t)^5}\right) + 2 & \text{if} \quad t_3 \le t < t_4 \\ \frac{10(t-t_4)^5}{\left((t-t_4)^5+(t_5-t)^5\right)+2} & \text{if} \quad t_4 \le t \le t_5 \end{cases}$$

$$z_d(t) = \begin{cases} \frac{10t^5}{\left(t^5+(t_1-t)^5\right)} & \text{if} \quad 0 \le t \le t_1 \\ 2\sin\left(\frac{(\pi/2)(t-t_1)^5}{(t-t_1)^5+(t_2-t)^5}\right)+10 & \text{if} \quad t_1 < t \le t_2 \\ 12 & \text{if} \quad t_2 < t \le t_5 \end{cases}$$

$$\psi_d(t) = \begin{cases} \psi_d(0) + \frac{D_\psi}{2\pi}\left[2\pi\frac{t}{t_5} - \sin\left(2\pi\frac{t}{t_5}\right)\right] & \text{if} \quad 0 \le t \le t_5 \\ \psi_d(t_5) & \text{if} \quad t > t_5 \end{cases}$$

with $D_\psi = \psi_d(t_5) - \psi_d(0)$ and t_1 = 16 s, t_2 = 26 s, t_3 = 45 s, t_4 = 55 s, t_5 = 140 s.

In the simulation, the H_∞-ANC controller parameters are chosen as follows: $\gamma_{f_{01}} = \gamma_{g_{01}} = \gamma_{f_{02}} = \gamma_{g_{02}} =$ 16, $\gamma_{f_{03}} = \gamma_{g_{03}} =$ 10, $\gamma_{f_{04}} = \gamma_{g_{04}} =$ 15, $\gamma_{f_{05}} = \gamma_{g_{05}} =$ 30, $\gamma_{f_{06}} = \gamma_{g_{06}} =$ 34, μ_i = 1. The attenuation level is set to: ρ_i = 0.695, i = (1, 2, ..., 6). The gains are chosen as K_i = (10, 10), i = (1, 2, 3), K_4 = (4.5, 4.5), K_5 = (1.75, 1.5), K_6 = (1.85, 1.5), $A_i = \begin{pmatrix} 0 & 1 \\ -10 & -10 \end{pmatrix}$, i = (1, 2, 3), $A_4 = \begin{pmatrix} 0 & 1 \\ -4.5 & -4.5 \end{pmatrix}$, $A_5 = \begin{pmatrix} 0 & 1 \\ -1.75 & -1.5 \end{pmatrix}$, $A_6 = \begin{pmatrix} 0 & 1 \\ -1.85 & -1.5 \end{pmatrix}$, $b_i = \begin{pmatrix} 0 \\ 1 \end{pmatrix}$, i = (1, 2, ..., 6) and the initial value of the state vector is X = [0, 0, 0, 0, 0, 0]^T. The matrices Q_i are chosen as diagonal matrices: $Q_1 = Q_2 = \begin{pmatrix} 660 & 0 \\ 0 & 660 \end{pmatrix}$, $Q_3 = \begin{pmatrix} 600 & 0 \\ 0 & 600 \end{pmatrix}$, $Q_4 = \begin{pmatrix} 580 & 0 \\ 0 & 580 \end{pmatrix}$, $Q_5 = \begin{pmatrix} 45 & 0 \\ 0 & 45 \end{pmatrix}$, $Q_6 = \begin{pmatrix} 53 & 0 \\ 0 & 53 \end{pmatrix}$. The linear matrix inequalities (42) give $P_1 = P_2 = \begin{pmatrix} 996.859 & 50.122 \\ 50.122 & 60.416 \end{pmatrix}$, $P_3 = \begin{pmatrix} 902.157 & 51.314 \\ 51.314 & 67.590 \end{pmatrix}$, $P_4 = \begin{pmatrix} 791.385 & 105.505 \\ 105.505 & 176.919 \end{pmatrix}$, $P_5 = \begin{pmatrix} 93.007 & 18.436 \\ 18.436 & 49.118 \end{pmatrix}$, $P_6 = \begin{pmatrix} 108.697 & 19.899 \\ 19.899 & 54.835 \end{pmatrix}$.

The controller parameters of H_∞-ANSMC are chosen as: The attenuation level is ρ_i = 0.1, i = (1, 2, ..., 6) and the sliding surfaces are chosen as follows: $S_1 = 10e_1 + 10\dot{e}_1$, $S_2 = 10e_2 + 10\dot{e}_2$, $S_3 = 10e_3 + 10\dot{e}_3$, $S_4 = 15e_4 + 5\dot{e}_4$, $S_5 = 8e_5 + 8\dot{e}_5$, $S_6 = 8e_6 + 7\dot{e}_6$, $\gamma_{f_{01}} = \gamma_{g_{01}}$ = 13, $\gamma_{f_{02}}$ = 10, $\gamma_{g_{02}}$ = 0.05, $\gamma_{f_{03}} = \gamma_{g_{03}}$ = 10, $\gamma_{f_{04}}$ = 3, $\gamma_{g_{04}}$ = 0.001, $\gamma_{f_{05}}$ = 5,$\gamma_{g_{05}}$ = 2, $\gamma_{f_{06}} = \gamma_{g_{06}}$ = 4. The parameter matrices Q_i are taken as diagonal matrices: $Q_1 = \begin{pmatrix} 75 & 0 \\ 0 & 70 \end{pmatrix}$, $Q_2 = \begin{pmatrix} 75 & 0 \\ 0 & 75 \end{pmatrix}$, $Q_3 = Q_5 = \begin{pmatrix} 65 & 0 \\ 0 & 65 \end{pmatrix}$, $Q_4 = \begin{pmatrix} 1 & 0 \\ 0 & 1 \end{pmatrix}$, $Q_6 = \begin{pmatrix} 30 & 0 \\ 0 & 30 \end{pmatrix}$, from equation (68), we have: $P_1 = \begin{pmatrix} 556.138 & 51.689 \\ 51.689 & 59.347 \end{pmatrix}$, $P_2 = \begin{pmatrix} 585.905 & 52.525 \\ 52.525 & 62.462 \end{pmatrix}$, $P_3 = \begin{pmatrix} 507.408 & 45.500 \\ 45.500 & 54.103 \end{pmatrix}$, $P_4 = \begin{pmatrix} 10.833 & 0.338 \\ 0.3386 & 0.7214 \end{pmatrix}$, $P_5 = \begin{pmatrix} 448.097 & 45.583 \\ 45.583 & 57.877 \end{pmatrix}$, $P_6 = \begin{pmatrix} 245.834 & 20.142 \\ 20.142 & 26.610 \end{pmatrix}$.

The initial values of the RBF weights have been set to 0.10. The number of hidden units for the RBF NNs is taken as 10. The structure of RBF is chosen for each subsystem as two input-ten hidden-one output. The centers $\eta_{f_0ij} = \eta_{g_0ij}$ = 5 are evenly distributed in the [1, –1] region and the variance is set as 15.

Figure 6 and 8 show the tracking of the desired trajectory and the stabilisation and motion of the quadrotor in 3D space. It can be seen that the translation motion of

the quadrotor achieved the desired trajectory. These simulation results demonstrate the effectiveness and tracking capability of the proposed robust controller for the quadrotor UAV. The propellers speeds are stabilised at 365 rad/s in a very short time as shown in Figure 7. The roll and pitch angles wave forms are shown in Figure 9. It can be observed that H_∞-ANSMC provides a more stable attitude variation. These results demonstrate that the proposed controller with H_∞-ANSMC leads to a better transient performance than the H_∞-ANC and the response is much smoother.

Figure 6 Global trajectory 1 of the quadrotor in (x, y, z) (see online version for colours)

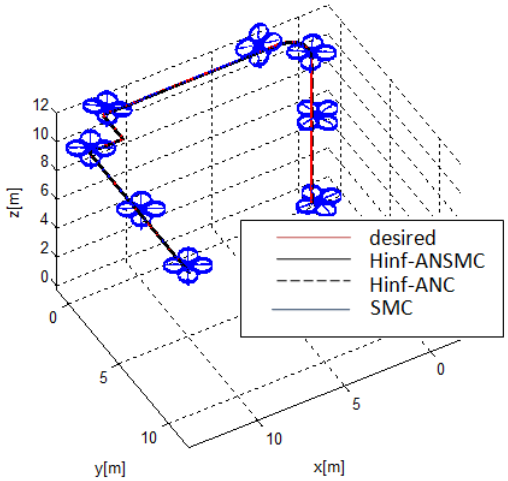

Figure 7 Angular velocities of the four rotors with H_∞-ANSMC under external disturbances and parameter uncertainties (see online version for colours)

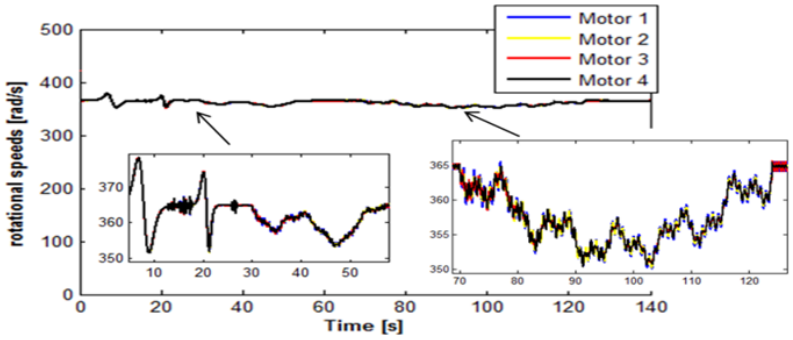

Figure 8 Outputs responses of the quadrotor (see online version for colours)

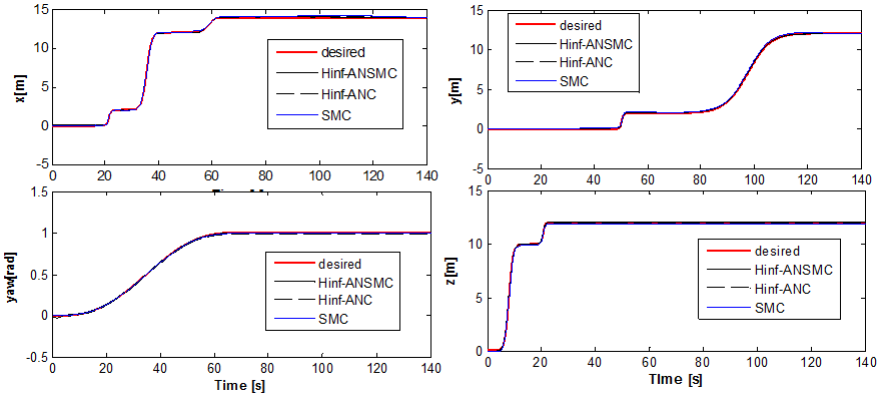

Figure 9 Roll (ϕ) and the pitch (θ) angles (see online version for colours)

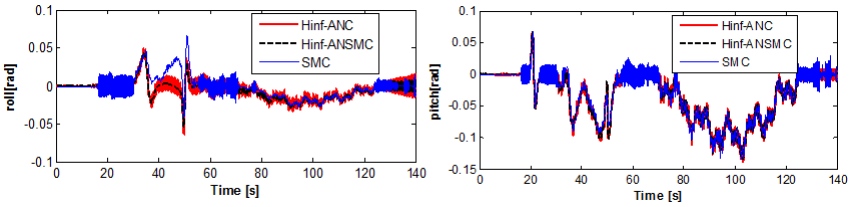

Figure 10 Forces control inputs (see online version for colours)

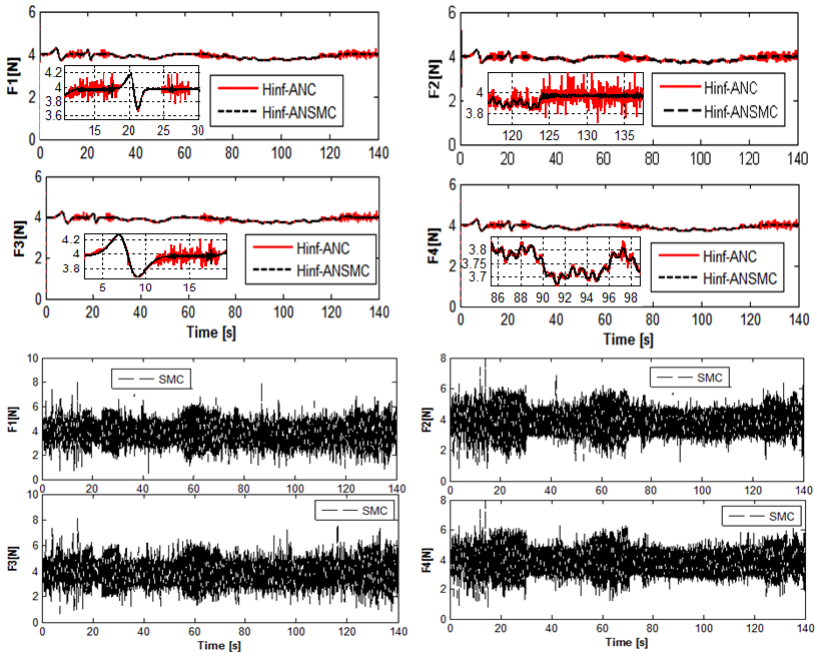

Figure 11 Quadrotor outputs errors (see online version for colours)

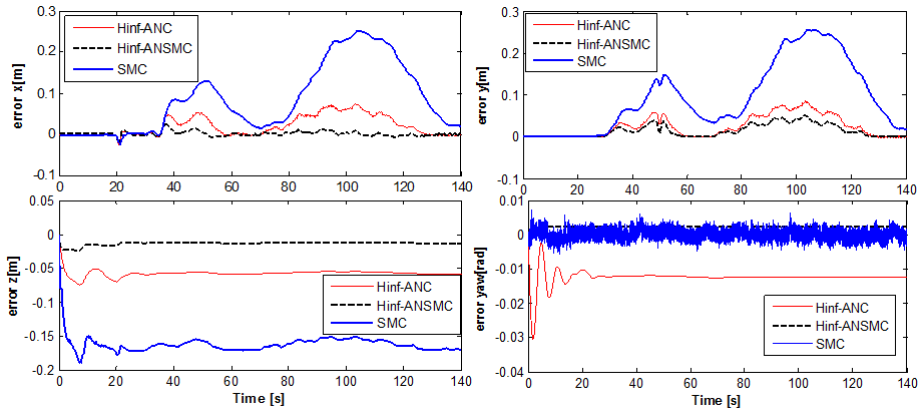

Figure 12 Trajectory of the sliding function of (x, y, z, ψ)

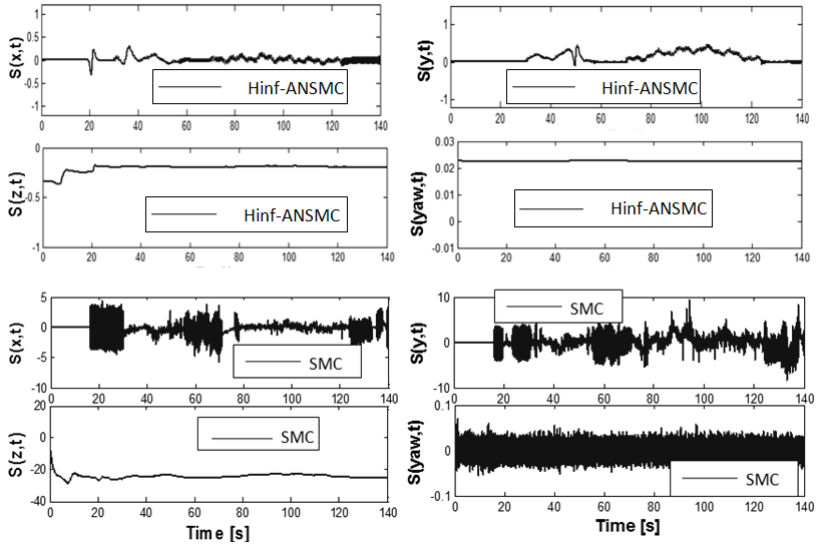

As shown in Figure 10, H_∞ based on adaptive neural SMC strategy generates a smooth input control signal as compared to others controllers and the required control forces under H_∞-ANSMC are smaller. The resulting tracking errors are shown in Figure 11. The proposed H_∞-ANSMC strategy provide a better tracking of the desired trajectory despite the presence of external disturbances (wind gust effect) and parametric uncertainties. The proposed H_∞-ANSMC proved to have a better tracking performance than H_∞-ANC.

The trajectory of the sliding function $s(t)$ is depicted in Figure 12 which clearly shows a reduction in the oscillations around the sliding surface. From the comparative results, it can be inferred that the H_∞-ANSMC reduces the chattering without compromising the transient characteristics.

Figure 13 Flight trajectory 2, (a) in three dimensions (b) $x - y$ plane (see online version for colours)

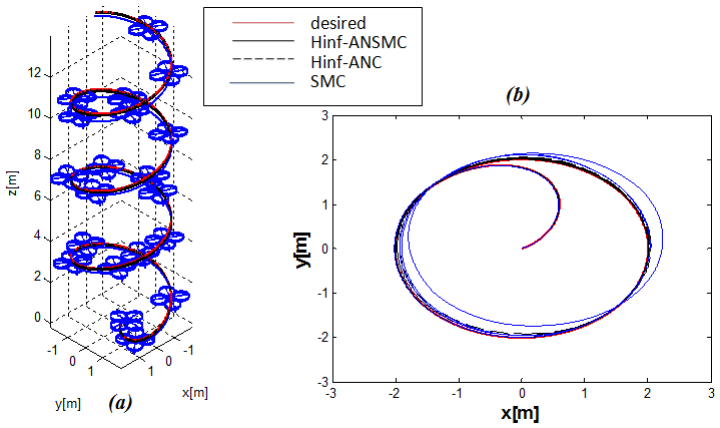

Figure 14 Outputs responses of the quadrotor (see online version for colours)

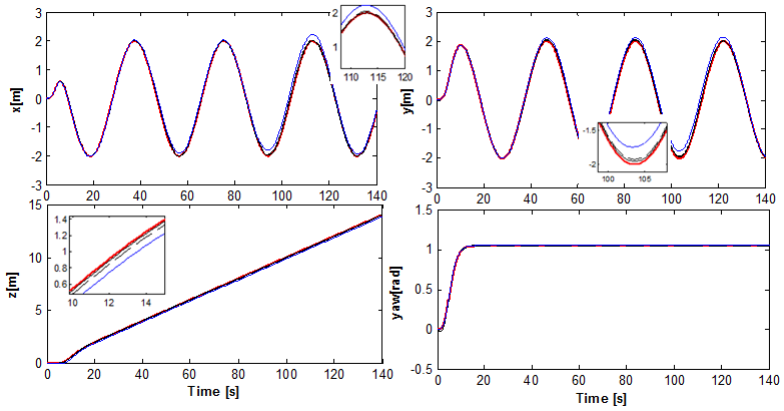

Figure 15 Roll (ϕ) and the pitch (θ) angles (see online version for colours)

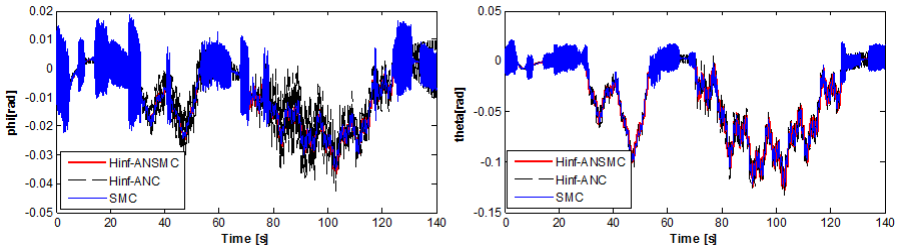

Another simulation result of the quadrotor trajectory in 3D space is presented in Figure 13. This result shows good trajectory tracking with both control strategies when the quadrotor is subjected to external disturbances and parameters uncertainties. As shown in Figure 17 the oscillations around the sliding surface much less than those

with SMC. Therefore, the simulation results demonstrate that H_∞-ANSMC trajectory tracking control scheme has better dynamic performance and stronger robustness against external disturbances and modelling errors as compared to the two control strategies.

Figure 16 Quadrotor outputs errors (see online version for colours)

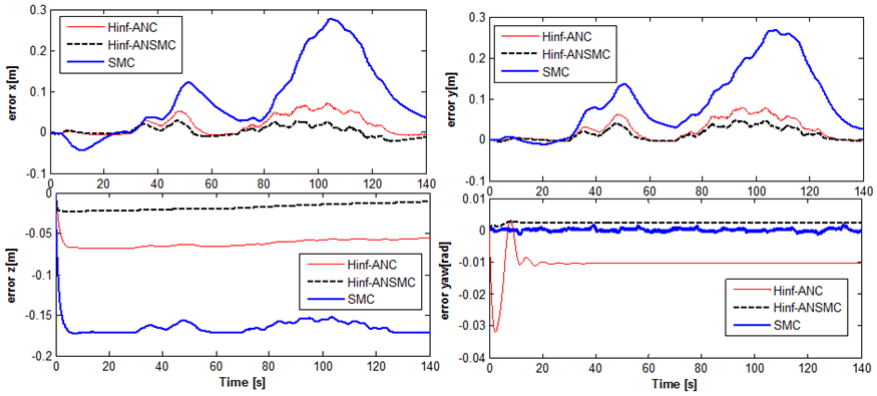

Figure 17 Trajectory of the sliding function of (x, y, z, ψ) (see online version for colours)

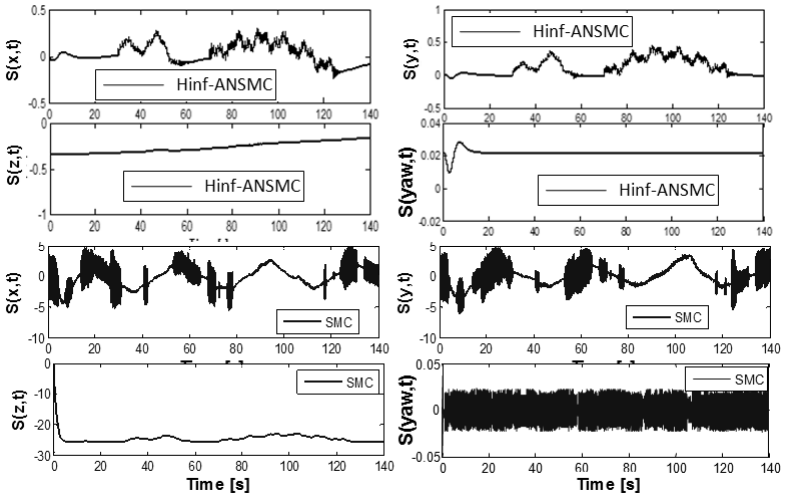

To quantify more explicitly the differences between these control methods, the following two criteria are used

1 The sums of the variances of the tracking errors (EV) in the (x, y, z, ψ) axis under external disturbances and parametric uncertainties.

2 The energy consumption (ECM) is the energy spent on motion control. This energy can be calculated from the sum of the motors squared angular speeds.

A comparison of three control methods with wind distrubance and parameter uncertainties is shown in Table 1. The proposed H_∞-ANSMC shows it advantage during wind distrubance and parameter uncertainties. The sum of the variance of the tracking errors of H_∞-ANSMC has the smallest error variance, while the other two controls, especially SMC, have larger tracking errors. The flight duration time depends on two factors: the capacity of the onboard battery and the energy consumption. Energy consumptions are not changed too much in H_∞-ANSMC and H_∞-ANC but for the case of SMC it is quite high. This is due to the switching feature of the SMC.

Table 1 Comparison of the proposed control methods

		H_∞-ANSMC	*H_∞-ANC*	*SMC*
Trajectory 1	$\boldsymbol{EV}$	0.0945	0.8015	7.264
	$\boldsymbol{ECM}$	7.286×10^7	7.288×10^7	7.295×10^7
Trajectory 2	$\boldsymbol{EV}$	0.1349	0.856	7.956
	$\boldsymbol{ECM}$	7.286×10^7	7.287×10^7	7.296×10^7

Remark 3: The neural approximation is only guaranteed within a compact set, there exists an adaptive controller with neural approximation such that all the closed-loop signals are bounded when the initial states are within this compact set. In practical control systems, the number of nodes usually cannot be chosen too large due to the possible computation problem. This implies that the RBF NNs approximation capability is limited. Namely, the larger the number of the nodes is, the more complexities the controller will contain. Therefore, the selection of the optimal number of hidden units still remains an open research problem.

7 Conclusions

In this paper two robust control strategy are proposed to solve the path tracking problem of a quadrotor helicopter taking into account wind disturbance and parameter variations which may influence the evolution of the system in space. The first controller combines H_∞ control strategy with an adaptive neural SMC algorithm. The advantage of this approach is that the dynamic model of the quadrotor is not required in the design of the controller. RBF NNs are used to approximate unknown functions to overcome the limitations of feedback linearisable techniques which need exact models. The RBF NNs weights adaptation laws have been derived to make the closed-loop system stable in the sense of Lyapunov under which the global stability of the proposed quadrotor adaptive flight control system is guaranteed. The simulation results show a good performance of the proposed control approach and good robustness with regard to parameter variations and external load disturbance. Future works will focus on improving our approach by introducing a state observer to provide an estimate of the state vector and association of an optimal trajectories generation algorithm with a flight control strategy.

Acknowledgements

The authors would like to thank the anonymous reviewers for any comments and suggestions that enhance the technical and scientific quality of this paper.

References

Amin, R.U. and Aijun, L. (2017) 'Design of mixed sensitivity H_∞ control for four-rotor hover vehicle', *Int. J. Automation and Control*, Vol. 11, No. 1, pp.89–103.

Anderson, B.D.O. and Moore, J.B. (1993) *Optimal Control: Linear Quadratic Methods*, Prentice Hall International, London.

Basri, M.A.M., Husain, A.R. and Kumerasan, A.D. (2015) 'Intelligent adaptive backstepping control for MIMO uncertain non-linear quadrotor helicopter systems', *Transactions of the Institute of Measurement and Control*, Vol. 37, No. 3, pp.345–361.

Behera, L. and Kar, I. (2010) *Intelligent Systems and Control: Principles and Applications*, Oxford University Press, New Delhi, India.

Besnard, L., Shtesse, Y.B. and Landrum, B. (2012) 'Quadrotor vehicle control via sliding mode controller driven by sliding mode disturbance observer', *Journal of the Franklin Institute*, Vol. 349, No. 1, pp.658–684.

Beyhan, S. and Ali, M. (2009) 'A new RBF network modeling based sliding mode control of nonlinear systems', *IEEE 4th International Symposium Advances in Artificial Intelligence and Applications*, Poland, pp.11–16.

Bouadi, H., Bouchoucha, M. and Tadjine, M. (2007) 'Sliding mode control based on backstepping approach for an UAV type-quadrotor', *International Journal of Applied Mathematics and Computer Sciences*, Vol. 4, No. 1, pp.12–17.

Boufadene, M., Belkheiri, M. and Rabhi A. (2018) 'Adaptive nonlinear observer augmented by radial basis neural network for a nonlinear sensorless control of an induction machine', *Int. J. Automation and Control*, Vol. 12, No. 1, pp.27–43.

Chen, B., Chang, Y. and Lee, T. (1997) 'Adaptive control in robotic systems with H_∞ tracking performance', *Automatic*, Vol. 33, No. 2, pp.227–234.

Chen, Y.M., He, Y.L. and Zhou, M.F. (2015) 'Decentralized PID neural network control for a quadrotor helicopter subjected to wind disturbance', *Journal of Central South University*, Vol. 22, No. 1, pp.168–179.

Chung, T.A. and Scarselli, F. (1998) 'Universal approximation using feedforward neural networks: a survey of some existing methods, and some new results', *Neural Networks: The Official Journal of the International Neural Network Society*, Vol. 11, No. 1, pp.15–37.

Devika, K.B. and Thomas, S. (2018) 'Improved reaching law-based sliding mode controller for free flight autopilot system', *Int. J. Automation and Control*, Vol. 12, No. 3, pp.361–380.

Emran, B.J. and Najjaran, H. (2017) 'Adaptive neural network control of quadrotor system under the presence of actuator constraints', *IEEE International Conference on Systems, Man, and Cybernetics (SMC)*, pp.2619–2624.

Haykin, S. (2009) *Neural Networks and Learning Machines*, 3rd ed., Pearson Prentice Hall, Upper Saddle River, New Jersey.

Horn, R.A. and Johnson, C.R. (1985) *Matrix Analysis*, Cambridge University Press, Cambridge.

Isidori, A. (1989) *Nonlinear Control Systems*, 2nd ed., Springer-Verlag, New York/Berlin.

Lanzon, A., Freddi, A. and Longhi, S. (2014) 'Flight control of a quadrotor vehicle subsequent to a rotor failure', *Journal of Guidance Control and Dynamics*, Vol. 37, No. 2, pp.580–591.

Liu, M. (2008) 'Robust H_∞ control for uncertain delayed nonlinear systems based on standard neural network models', *Neurocomputing*, Vol. 71, Nos. 16–18, pp.3469–3492.

Long, F. and Fei, S.M. (2008) 'Neural networks stabilization and disturbance attenuation for nonlinear switched impulsive systems', *Neurocomputing*, Vol. 71, Nos. 7–9, pp.1741–1747.

Madani, T. and Benallegue, A. (2007) 'Sliding mode observer and backstepping control for a quadrotor unmanned aerial vehicles', *Proceedings of the 2007 American Control Conference IEEE*, pp.5887–5892.

Maiti, R., Sharma, K.D. and Sarkar, G. (2018) 'PSO based parameter estimation and PID controller tuning for 2-DOF nonlinear twin rotor MIMO system', *Int. J. Automation and Control*, Vol. 12, No. 4, pp.582–609.

Mellouli, E.M., Alfidi, M. and Boumhidi, I. (2018) 'Fuzzy sliding mode control for three-tank system based on linear matrix inequality', *Int. J. Automation and Control*, Vol. 12, No. 2, pp.237–250.

Mohammadi, M. and Shahri, A.M. (2013) 'Adaptive nonlinear stabilization control for a quadrotor UAV: theory, simulation and experimentation', *Journal of Intelligent and Robotic Systems*, Vol. 72, No. 1, pp.105–122.

Mokhtari, A., Benallegue, A. and Daachi, B. (2005) 'Robust feedback linearization and GH_∞ controller for a quadrotor unmanned aerial vehicle', *IEEE/RSJ International Conference on Intelligent Robots and Systems*, pp.1198–1203.

Ozbek, N.S., Onko, M. and Efe, M.O. (2015) 'Feedback control strategies for quadrotor-type aerial robots: a survey', *Transactions of the Institute of Measurement and Control*, Vol. 38, No. 5, pp.529–554.

Shakev, N.G. and Topalov, A.V. (2015) 'Continuous sliding mode control of a quadrotor', *Recent Advances in Sliding Modes: From Control to Intelligent Mechatronics. Studies in Systems, Decision and Control*, Vol. 24, pp.441–458, Springer.

Sira-Ramírez, H. (2015) *Sliding Mode Control: The Delta Sigma Modulation Approach*, Birkhäuser Basel, Springer International Publishing, Switzerland.

Slotine, J.J.E. and Li, W. (1991) *Applied Nonlinear Control*, Prentice-Hall, Englewood Cliffs, New Jersey.

Talha, M., Asghar, F., Rohan, A., Rabah, M. and Kim, S.H. (2018) 'Fuzzy logic-based robust and autonomous safe landing for UAV quadcopter', *Arabian Journal for Science and Engineering*, pp.1–13, Springer [online] https://doi.org/10.1007/s13369-018-3330-z.

Tayebi, A. and McGilvray, S. (2006) 'Attitude stabilization of a VTOL quadrotor aircraft', *IEEE Transactions on Control Systems Technology*, Vol. 14, No. 3, pp.562–571.

Wang, D.L., Qiang, L. and Liu, F. (2012) 'Quadrotor attitude control based on L_1 neural network adaptive control method', *Comput Eng Des*, Vol. 33, No. 12, pp.4758–4761.

Wang, L. (1989) 'Stable adaptive fuzzy control of nonlinear systems', *IEEE Transactions on Fuzzy Systems*, Vol. 1, No. 2, pp.146–155.

Yacef, H.F., Bouhali, H., Khebbache, H. and Boudjema, F. (2012) 'Takagi-Sugeno model for quadrotor modelling and control using nonlinear state feedback controller', *International Journal of Control Theory and Computer Modelling*, Vol. 2, No. 3, pp.9–24.

Yu, L., Fei, S.M. and Li, X. (2010) 'Robust adaptive neural tracking control for a class of switched affine nonlinear systems', *Neurocomputing*, Vol. 73, pp.2274–2279.

Zhang, Y., Xu, B. and Li, H. (2015) 'Adaptive neural control of a quadrotor helicopter with extreme learning machine', *Proceedings in Adaptation, Learning and Optimization*, Vol. 4, pp.125–134, Springer.

Appendix

Table 2 The quadrotor model parameters

Symbol	*Definition*	*Value*
M	Mass	0.486 kg
I_x	Inertia on x axis	7.656×10^{-3} kg m^2
I_y	Inertia on y axis	3.826×10^{-3} kg m^2
I_z	Inertia on z axis	3.826×10^{-3} kg m^2
b	Thrust coefficient	2.9842×10^{-5} N/rad/s
d	Drag coefficient	$3{,}232 \times 10^{-5}$ N/rad/s
J_r	Rotor inertia	2.8385×10^{-5} kg m^2
K_{fax}, K_{fay}	Friction coefficients	5.567×10^{-4} N/rad/s
K_{faz}	Friction coefficient	6.354×10^{-4} N/rad/s
K_{ftx}, K_{fty}	Drag coefficients	$5{,}567 \times 10^{-4}$ N/m/s
K_{ftz}	Drag coefficient	6.354×10^{-4} N/m/s
l	Arm length	0.25 m